AECL-8342

ATOMIC ENERGY OF CANADA LIMITED

L'ÉNERGIE ATOMIQUE DU CANADA LIMITÉE

DESIGN OF A MULTIVARIABLE CONTROLLER FOR A CANDU 600 MWe NUCLEAR POWER PLANT USING THE INA METHOD

Conception d'un système de commande et de régulation pour une centrale nucléaire CANDU 600 MWe avec la méthode INA

N. ROY, S. MENSAH and J. BOISVERT

Chalk River Nuclear Laboratories

Laboratoires nucléaires de Chalk River

Chalk River, Ontario

April 1984 avril

ATOMIC ENERGY OF CANADA LIMITED

DESIGN OF A MULTIVARIABLE CONTROLLER FOR A CANDU 600 MWe NUCLEAR POWER PLANT USING THE INA METHOD

by

N. Roy*, S. Mensah and J. Boisvert*

*Ecole Polytechnique de Montréal

Chalk River Nuclear Laboratories
Chalk River, Ontario K0J 1J0

1984 April

AECL-8342

L'ENERGIE ATOMIQUE DU CANADA LIMITEE

CONCEPTION D'UN SYSTEME DE COMMANDE ET DE REGULATION POUR UNE CENTRALE NUCLEAIRE CANDU 600 MWe AVEC LA METHODE INA

par

N. Roy*, S. Mensah et J. Boisvert*

SOMMAIRE

Le développement des complexes industriels nécessite l'utilisation de systèmes de contrôle très performants, conçus avec des techniques multivariables.

Ce travail fait partie d'une série d'études analytiques visant à démontrer le potentiel réel des méthodes multivariables. Il comprend toutes les étapes de la conception d'un contrôleur multivariable pour une centrale nucléaire CANDU 600 MWe du type Gentilly-2, avec l'utilisation de la méthode de la matrice inversée de Nyquist (INA).

Le modèle linéaire utilisé dans la conception du contrôleur et les modifications préliminaires requises sont décrits. Ensuite, les outils de conceptions et les opérations effectuées pour obtenir la dominance diagonale du système en boucle ouverte sont systématiquement décrits. L'analyse du système en boucle fermée conduit au choix d'une matrice de rétroaction qui respecte les spécifications. La performance du contrôleur sur le modèle linéaire est vérifiée par simulation. Enfin, le contrôleur est implanté sur le modèle non linéaire et l'évaluation de ses performances est effectuée par voie de simulation.

Les résultats démontrent que la méthode INA peut être utilisée avec succès dans la conception d'un contrôleur pour un système industriel complexe.

---

*Ecole Polytechnique de Montréal

Laboratoires nucléaires de Chalk River
Chalk River, Ontario K0J 1J0

1984 Avril

AECL-8342

ATOMIC ENERGY OF CANADA LIMITED

DESIGN OF A MULTIVARIABLE CONTROLLER FOR A CANDU 600 MWe NUCLEAR POWER PLANT USING THE INA METHOD

by

N. Roy*, S. Mensah and J. Boisvert*

ABSTRACT

The development of large and complex nuclear and process plants requires high-performance control systems, designed with rigourous multivariable techniques.

This work is part of an analytical study demonstrating the real potential of multivariable methods. It covers every step in the design of a multivariable controller for a Gentilly-2 type CANDU 600 MWe nuclear power plant, using the Inverse Nyquist Array (INA) method.

First of all, the linear design model and its preliminary modifications are described. The design tools are reviewed and the operations required to achieve open-loop diagonal dominance are thoroughly described. Analysis of the closed-loop system is then performed and a feedback matrix is selected to meet the design specifications. The performance of the controller on the linear model is verified by simulation. Finally, the controller is implemented on the reference non-linear model to assess its overall performance.

The results show that the INA method can be used successfully to design controllers for large and complex systems.

---

*Ecole Polytechnique de Montreal

Chalk River Nuclear Laboratories
Chalk River, Ontario K0J 1J0

1984 April

AECL-8342

TABLE OF CONTENTS

TABLE OF CONTENTS (cont'd)

NOMENCLATURE

Symbol	Description	Defining Equation
A	Plant dynamics matrix	(1)
A_c	Controller state matrix	(25)
B	Plant input matrix	(1)
B_c	Controller input matrix	(25)
C	Plant output matrix	(2)
C_c	Controller output matrix	(24)
C_1, C_2, C_{i1}, C_{i2}	Contours	-
$d_i(s)$	Gershgorin radius	(14)
D	Nyquist contour	-
D	Plant input-output coupling matrix	(2)
D_c	Controller matrix for G2SIM, general form	(24)
e	Error vector	-
f	Element of feedback gain matrix	-
fI	Element of FI	-
FI	Inverse of F	-
F(s),F	Feedback matrix	(4)
GI(s)	Inverse of G(s)	(5)
G(s)	Open-loop transfer function matrix	(3)
hI	Element of HI	-

NOMENCLATURE (cont'd)

Symbol	Description	Defining Equation
HI(s)	Inverse of H(s)	(6)
H(s)	Closed-loop transfer function matrix	(4)
k	Dimensions of QI	-
K*	Controller matrix	(22)
KI_o	Inverse of K_o	(21)
KI(s)	Inverse of K(s)	(5)
K_o	Initial pre-compensator	(20)
K(s)	Pre-compensator matrix	(3)
$L_D(t)$	Level in steam drum	-
LI_o	Inverse of L_o	(21)
LI(s)	Inverse of L(s)	(5)
L_o	Initial post-compensator	(20)
$L_p(t)$	Level in pressurizer	-
L(s)	Post-compensator matrix	(3)
n(t)	Reactor power	-
N_1, N_2, N_{i1}, N_{i2}	Number of encirclements of the origin	-
P_o	Number of unstable poles	(8)

NOMENCLATURE (cont'd)

Symbol	Description	Defining Equation
$P_D(t)$	Pressure in steam drum	-
$P_M(t)$	Turbine mechanical power	-
$P_{ROH}(t)$	Pressure in reactor outlet header	-
$P_S(t)$	Pressure in pressurizer	-
qI	Element of QI	(9)
$Q_H(t)$	Power dissipated by surge tank heaters	-
QI(s)	Inverse of Q(s)	(5)
Q(s)	Compensated open-loop transfer function matrix	(3)
r	Setpoint vector	-
r'	Setpoint vector	(26)
$r_i(s)$	Dominance ratio	(19)
s	Laplace-transform variable	-
$S_{FW}(t)$	Feedwater valve demand opening	-
$S_s(t)$	Governor valve opening	-

NOMENCLATURE (cont'd)

Symbol	Description	Defining Equation
$S_z(t)$	Demanded zone control valve position	-
t	Time	-
$u(t)$	Input vector	(1)
$u'(t)$	Modified input vector	-
u_k	Discretized input vector	(23)
$U_{PROH}(t)$	Heavy water feed or bleed flow	-
$W_s(t)$	Boiler outlet steam flow	-
$W_F(t)$	Feedwater flow	-
$x(t)$	State vector	(1)
$y(t)$	Output vector	(2)
$y'(t)$	Modified output vector	-
z	Output vector	-
Greek Letters		
α	State vector of the controller	(23)
α	Constant	-
Δ	Change	-
$\phi_i(s)$	Ostrowski factor	(16)
λ	Eigenvalue	-
θ	Stability phase margin	-
$\theta_i(s)$	Dominance ratio	(15)
ω	Imaginary part of eigenvalue	-
σ	Real part of eigenvalue	-

LIST OF FIGURES

LIST OF TABLES

1. INTRODUCTION

The operation of large and complex nuclear and process plants closer to maximum capacity requires high-performance control systems. These plants are multivariable systems with strong interactions and thus cannot be rigorously analyzed with traditional scalar methods. Multivariable techniques can handle the simultaneous analysis of several plant variables, potentially allowing system performance specifications to be met directly, during the controller design process [1].

At the Chalk River Nuclear Laboratories (CRNL), applications of multivariable techniques to the regulation of CANDU* nuclear power plants has been under study for the last few years [2]. This project is part of an analytical study demonstrating the real potential of multivariable methods. The objective is to apply Rosenbrock's [3] Inverse Nyquist Array (INA) method to design a controller for a non-linear and complex model of a CANDU 600 MWe nuclear power plant [4].

The characteristics of the design model used in this study are described in Section 2. The underlying theory of the INA method is briefly reviewed in Section 3. The procedures followed to design the controller are explained in Section 4. The implementation and the performance of the controller on the non-linear model are discussed in Section 5.

2. DESIGN MODEL

2.1 Introduction

The linear design model used in this study was derived from G2SIM [4]. G2SIM is a simulation program developed to study the overall performance of the regulating system of Gentilly-2 nuclear power plant. A real time version is implemented on a PDP-11/55 digital computer of the Dynamic Analysis Laboratory at CRNL. All the major subsystems of the plant have been modelled: the primary circuit including the reactor, the primary coolant and the pressurizer, the steam generators, and the secondary circuit including the feedwater circuit and the turbine.

2.2 Derivation of the Linear Model

G2SIM is a fairly large non-linear model and it cannot be used directly by most multivariable control design methods. A linear model derived from G2SIM was developed for control system design purposes.

Before the linearization, the G2SIM model was simplified using the following approximations and assumptions:

- the reactor dynamics are approximated by a point kinetics model with two delayed neutron groups and one average decay heating group,

---

*CANada Deuterium Uranium

- heat transfer in the fuel is modelled by an average fuel temperature derived from a two-shell model,
- valve dynamics are neglected,
- time delays are neglected or replaced by first-order lags,
- volume of steam in boiler riser is constant,
- the dynamics of the turbine power are approximated by a first-order lag.

The simplified non-linear model obtained is then linearized about a steady state operating condition using small perturbation theory. The resulting linear design model called G2LDM (G2 Linear Design Model) [2] can be described by the state-space equations

$$\dot{x}(t) = Ax(t) + Bu(t) \qquad (1)$$

$$y(t) = Cx(t) + Du(t) \qquad (2)$$

where

x(t) is the state vector, of dimension 24
u(t) is the input vector, of dimension 5
y(t) is the output vector, of dimension 8

The matrices A, B, C and D, calculated from full-power data, are shown in Appendix 1 with the open-loop eigenvalues.

The input variables are:

u_1 : Demanded zone control valve position, $\Delta S_z(t)$

u_2 : Power dissipated in surge tank heaters, $\Delta Q_H(t)$

u_3 : Feed or bleed flow of heavy water, $\Delta U_{PROH}(t)$

u_4 : Feedwater valve demand opening, $\Delta S_{FW}(t)$

u_5: Governor valve opening, $\Delta S_s(t)$

The output variables are:

y_1 : Variation of neutron flux, $\Delta n(t)$

y_2 : Variation of reactor outlet header pressure, $\Delta P_{ROH}(t)$

y_3 : Variation of surge tank (pressurizer) level, $\Delta L_p(t)$

y_4 : Variation of boiler drum level, $\Delta L_D(t)$

y_5 : Variation of boiler drum pressure, $\Delta P_D(t)$

y_6 : Variation of difference between steam flow from boiler and feedwater flow, $\Delta W_s(t) - \Delta W_F(t)$

y_7 : Variation of turbine mechanical power, $\Delta P_M(t)$

y_8 : Variation of surge tank (pressurizer) pressure, $\Delta P_s(t)$

2.3 Initial Modifications of the Design Model

With 5 inputs and 8 outputs, the open-loop transfer-function matrix of G2LDM is not square, and cannot be directly inverted. For application of the INA method, the transfer-function matrix must be squared down by selection of 5 appropriate linear combinations of the 8 measurements. The final choice, based on engineering judgments, is

$$y_1' = y_1$$

to keep the reactor power measurement clean,

$$y_2' = y_5 - 5y_7$$

to take into account power imbalance between primary and secondary circuit,

$$y_3' = y_4 - y_6$$

to combine flow and level errors,

$$y_4' = y_2 - y_8$$

to respond to pressure imbalance between surge tank and primary circuit,

$$y_5' = y_3$$

to decouple surge tank level control loop from other measurements.

The input vector has also been scaled and reordered as follows:

$$u_1' = 10\ u_1$$

$$u_2' = 10\ u_5$$

$$u_3' = 10\ u_4$$

$$u_4' = 10000\ u_2$$

$$u_5' = 10\ u_3$$

where u_1' to u_5' are the new inputs.

3. THE INA METHOD

3.1 Introduction

The INA method, based on frequency responses, serves as a guide during the design of compensators which will sufficiently reduce the interaction between loops so that classical methods can be applied. The method can also be used to investigate the stability of the multivariable system. The underlying theory, developed by Rosenbrock [3], is briefly reviewed in the next sections.

3.2 Inverse Transfer Function

The most general model used to describe the closed-loop, multivariable system for the INA method is shown in Figure 3.1.

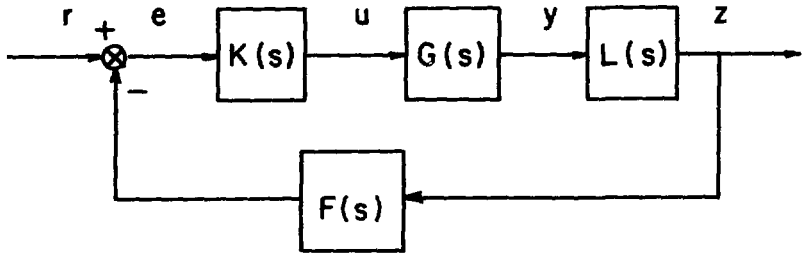

FIGURE 3.1 GENERAL INA DESIGN MODEL

G(s) is the transfer-function matrix describing the plant, K(s) and L(s) are the compensators and F(s) is the feedback matrix. u and e are the input and error vectors, while y and z are the output vectors and r is the reference vector.

Let Q(s) be the open-loop transfer-function matrix, and H(s), the closed-loop transfer-function matrix. Then, according to Figure 3.1,

$$Q(s) = L(s) \cdot G(s) \cdot K(s) \tag{3}$$

and

$$H(s) = [I + Q(s)F(s)]^{-1} \cdot Q(s) \tag{4}$$

It is assumed that Q(s) is a square and non-singular matrix. In the following, the inverse of a matrix "W" is expressed as "WI". From equations (1) and (2), the inverses of Q(s) and H(s), denoted by QI(s) and HI(s), are

$$QI(s) = KI(s) \cdot GI(s) \cdot LI(s) \tag{5}$$

and

$$HI(s) = QI(s) \cdot [I + Q(s)F(s)] \tag{6}$$

or

$$HI(s) = QI(s) + F(s) \tag{7}$$

where HI(s) is found by simply adding matrix F(s) to matrix QI(s).

3.3 Stability Criteria

The stability of the closed-loop system can be investigated by using the Nyquist criterion. This criterion gives the stability margin of the system and indicates how to improve stability. The Nyquist criterion is based on the following theorem.

Theorem 1

Let D be a large contour in the s-plane, consisting of the imaginary axis from -iR to +iR, together with a semicircle of radius R in the right

half-plane. Every finite zero and pole of $|QI|$ and $|HI|$ lying in the right half-plane must be included in the contour D. D must also be indented into the left half-plane to enclose any imaginary pole and zero of $|QI|$ and $|HI|$.

As s goes once clockwise around D, let $|QI|$ and $|HI|$ form respectively contours C_1 and C_2 and let C_1 and C_2 make N_1 and N_2 clockwise encirclements of the origin. Then, the closed-loop system is asymptotically stable if and only if

$$N_1 - N_2 = p_o \tag{8}$$

where p_o is the number of poles of the open-loop system in the right half complex plane [3, p. 141].

This stability criterion is difficult to use. It identifies stable systems, but when a system is unstable, the criterion fails to provide guidance in the choice of a feedback matrix F(s) which will stabilize the closed-loop system. Also, modifying the gain in one loop may perturb other loops through interaction.

This problem could be solved by making QI and F(s) diagonal matrices. But it may be very difficult or impossible to diagonalize QI. Rosenbrock has shown that the much looser criterion of diagonal dominance can be used.

3.4 Diagonal Dominance

3.4.1 Definition

The matrix QI, of dimensions k x k, is diagonally row dominant on D if

$$|qI_{ii}(s)| > \sum_{\substack{j=1 \\ j\neq i}}^{k} |qI_{ij}(s)| \tag{9}$$

for i = 1,2,...,k
and all s on D.

Also, it is diagonally column dominant on D if

$$|qI_{ii}(s)| > \sum_{\substack{j=1 \\ j\neq i}}^{k} |qI_{ji}(s)| \qquad (10)$$

for i = 1,2,...,k
and all s on D.

where qI_{ii} are the diagonal elements of QI, and where qI_{ij}, are the off-diagonal elements of QI. Ql is said to be diagonally dominant if it is either row or column dominant.

Diagonal dominance, or dominance, means that each diagonal element is greater in magnitude than the sum of the magnitudes of the corresponding off-diagonal terms.

3.4.2 Diagonal Dominance and Stability

The use of the concept of dominance in stability analysis of complex systems is based on the following theorem.

Theorem 2

Let QI be dominant on D; let qI_{ii} map D into C_{il}, with i=1,2,....k. Also, let $|QI|$ map D into C_l. Let C_{il} encircle the origin N_{il} times, and C_l encircle the origin N_l times (clockwise). Then

$$N_l = \sum_{i=1}^{k} N_{il} \qquad (11)$$

This theorem provides the foundation for the following stability theorems.

Theorem 3

Let F = diag (f_i), where the f_i are real and non-zero, and [FI + Q(s)], a dominant matrix on D. Let q_{ii} map D into C_{il} which encircles the point ($-fI_i$,0) N_{iI} times, i=1,2,...,k. Then the closed-loop system is asymptotically stable if and only if

$$\sum_{i=1}^{k} N_{il} = -p_o \qquad (12)$$

with p_o defined as previously.

Theorem 4

Let QI and HI be dominant on D. Let qI_{ii} map D into C_{i1} which encircles the origin N_{i1} times, and hI_{ii} map D into C_{i2} which encircles the origin N_{i2} times; then, the closed-loop system is asymptotically stable if and only if

$$\sum_{i=1}^{k} N_{i1} - \sum_{i=1}^{k} N_{i2} = p_o \qquad (13)$$

Matrix dominance can be verified graphically, by using the Gershgorin bands.

3.5 Gershgorin Bands

Let qI_{ii} map D into C_{i1}. Then select a value of s, and, at the corresponding point $qI_{ii}(s)$ on C_{i1} as centre, draw a circle of radius

$$d_i(s) = \sum_{\substack{j=1 \\ j\neq i}}^{k} |qI_{ij}(s)| \qquad (14)$$

As s goes around D, the corresponding circles sweep out a band, called the Gershgorin band. If the band formed by the set of circles excludes the origin in the qI_{ii} plane, the row i of QI is dominant on D. If each row is dominant on D, then QI is diagonally row dominant on D. The same procedure can be applied to columns.

An important theorem, which shows that smaller interactions exist between loops when QI is dominant, completes the graphical analysis.

3.6 Ostrowski Theorem

This theorem allows treatment of the stability problem as if the dominant system was made of non-interactive loops.

With HI dominant on D, define

$$\theta_i(s) = \frac{d_i(s)}{|hI_{ii}(s)|} \qquad (15)$$

where

$$d_i(s) = \sum_{\substack{j=1 \\ j\neq i}}^{k} |hI_{ij}(s)|$$

By definition,

$$\theta_i(s) < 1 \qquad \text{for all } s \text{ on } D.$$

Define also

$$\phi_i(s) = \max_{j,j\neq i} \theta_j(s) \tag{16}$$

where j is associated with the least dominant row of HI, excluding row i.

Then

$$|hI_{ii}(s) - h^{-1}_{ii}(s)| < \phi_i(s)\cdot d_i(s) < d_i(s) \tag{17}$$

for all i and all s on D.

This result shows that the element $h^{-1}{}_{ii}(s)$, which is the inverse transfer function seen between input i and output i, is included inside the Gershgorin band, and also inside a narrower band called the Ostrowski band, formed by a set of circles of radius $\phi_i(s)\cdot d_i(s)$.

Then, if QI and HI are dominant on D, any combination of gains in loops other than loop i keeps $h^{-1}{}_{ii}(s)$ in the Ostrowski band.

Ostrowski bands also locate $h^{-1}{}_{ii}(s)$, evaluated for $f_i=0$, in order to design a compensator for loop i, and they indicate the stability margin of the loops. Several techniques can be used to achieve dominance of the system, and are briefly presented here.

3.7 Achieving Dominance

Dominance of QI can usually be achieved with the appropriate compensators KI and LI. However, it is desirable to use simple compensators. In many cases static compensators are sufficient to achieve dominance.

Many techniques can be used to achieve dominance. A simple way is to apply a sequence of elementary operations, for example permuting rows (or columns) or scaling a row (or a column) with a constant, in order to place large entries on the diagonal.

Static compensators may not always achieve dominance [5]. Then, a choice of dynamic matrices KI(s) and/or LI(s) is necessary, with certain restrictions [3, p. 156].

Optimization methods can also be used, like pseudo-diagonalization [3, p. 162], which minimizes the sum

$$\sum_{\substack{j=1 \\ j\neq i}}^{k} |\, qI_{ij}(s)|^2 \qquad (18)$$

or the hillclimb algorithm [6], which minimizes the dominance ratio

$$r_i(s) = \frac{d_i(s)}{|qI_{ii}(s)|} \qquad (19)$$

where

$$d_i(s) = \sum_{\substack{j=1 \\ j\neq i}}^{k} |qI_{ij}(s)|$$

4. CONTROLLER DESIGN

4.1 Controller Specifications

The controller must be designed to meet the following specifications:

(1) Stability. The closed-loop system should be asymptotically stable, that is, all poles of the closed-loop system should lie in the open left half-plane.

(2) Stability margin. Let λ be a pole of the closed-loop system such that $\lambda = -\sigma \pm i\omega$; then the angle $\theta = \tan^{-1} \sigma/\omega$ is a measure of the stability margin. Indeed, over a period $2\pi/\omega$, the damped oscillation has a decrement equal to $\exp(-2\pi\sigma/\omega)$. θ should be larger than 45° (or $\sigma > \omega$).

(3) Overshoot. When a step input is applied to the system, the output will usually overshoot its final value, settling to it with a damped oscillation. This overshoot should be strictly controlled so that the output variables stay always inside the defined limits.

(4) Speed of response. The time taken for the system to respond to a step input indicates how effectively it will follow changes of the inputs. Because speed of response depends on the position of the dominant poles, these poles should not be too close to the origin.

(5) Sensitivity. The system's response should be insensitive to small perturbations or system parameter changes.

4.2 Design Tools

The controller has been designed within the framework provided by MVPACK, a package for computer-aided design of control systems [7].

The INA module of MVPACK [8] is used to investigate and achieve dominance. This interactive module allows the designer to use elementary operations as well as an optimization-based algorithm to drive the transfer function matrices toward dominance. The commands used to operate the INA module are summarized in Table 1.

TABLE 1

INA COMMANDS

Command	Description
ROW P,i,j	Permutation of rows i and j
ROW S,i,α	Scaling row i with a constant, α
ROW A,i,j,α	Adding α times row j to row i
ROW C,i	Application of Rosenbrock's hill-climbing algorithm on row i
ROW NAME,I	Premultiply QWI by matrix NAME (invert NAME if I specified)
QZE	Apply QW(0) to QWI
NYQ	Plot Nyquist plots

The COL command has the same options as the ROW command, applied to columns instead of rows.

After each operation, a list is displayed on the terminal. This list indicates the worst dominance ratio of each row (or each column) with the corresponding frequency and the number of frequencies for which dominance

is not obtained. Then, the designer may retain or reject the operation. If it is accepted, the corresponding compensator matrix is automatically calculated and saved.

The command NYQ calls the MVNYQ module [8] of MVPACK. This module plots, on a Tektronix 4663 plotter, the Nyquist diagrams for the inverse transfer-function matrix, with the Gershgorin or Ostrowski bands. This program provides graphical output which the designer would use to design compensators KI and LI and also choose a feedback matrix for the closed-loop system.

The poles are calculated with the use of the modules MVCAL and MVEIG [8]. The simulation of the closed-loop system is done with the modules MVSIM and MVRSIM [8].

4.3 Open-Loop Dominance Analysis

4.3.1 General

The modifications made to the model in Section 2.3 can be expressed as two initial compensators such that the open-loop transfer-function matrix is (Figure 4.1):

$$Q(s) = L_o \cdot G(s) \cdot K_o \qquad (20)$$

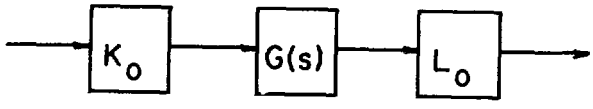

FIGURE 4.1 INITIAL MODIFICATIONS OF THE DESIGN MODEL

where

$$K_o = \begin{bmatrix} 10 & 0 & 0 & 0 & 0 \\ 0 & 0 & 0 & 10000 & 0 \\ 0 & 0 & 0 & 0 & 10 \\ 0 & 0 & 10 & 0 & 0 \\ 0 & 10 & 0 & 0 & 0 \end{bmatrix}$$

$$L_o = \begin{bmatrix} 1 & 0 & 0 & 0 & 0 & 0 & 0 & 0 \\ 0 & 0 & 0 & 0 & 1 & 0 & -5 & 0 \\ 0 & 0 & 0 & 1 & 0 & -1 & 0 & 0 \\ 0 & 1 & 0 & 0 & 0 & 0 & 0 & -1 \\ 0 & 0 & 1 & 0 & 0 & 0 & 0 & 0 \end{bmatrix}$$

The inverse of the open-loop transfer function matrix is expressed as

$$QI(s) = KI_o \cdot GI(s) \cdot LI_o \qquad (21)$$

As stated in Section 3, the dominance analysis for the open-loop system is based on the graphical construction of INA and Gershgorin circles of QI(s) (equation 5). For the case under study, the analysis proceeds in two steps. First, the dominance search is performed in the frequency band from 0.01 to 1.0 Hz, for 20 points. The results are then investigated in the same frequency band for 100 points.

The Gershgorin circles are plotted only on the diagonal elements. When the band formed by these circles does not include the origin, the corresponding row is dominant. A boundary circle is drawn for each element with an associated number on its right. This number gives the magnitude of the element at the boundary circle, and, therefore, may provide guidance for improving dominance.

4.3.2 First Step

Figure 4.2 shows the INA plot with the Gershgorin circles for the inverse of the open-loop transfer function matrix described in equation (21). Table 2 indicates the worst dominance ratio for each row with the corresponding frequency and the number of frequencies for which the row is not dominant. Only rows 1 and 2 are dominant. After many trials, it was found that QI(s) can be made diagonally dominant by driving the design module INA through the following sequential operations.

TABLE 2

DOMINANCE RATIOS, NO COMPENSATORS

ROW	DOM RATIO	FREQUENCY	NB FREQ
1	0.24	0.010	0
2	0.38	0.010	0
3	2.3	1.00	13
4	23.0	1.00	18
5	5.8	0.010	5

Sequence 1

Objectives: improve dominance on rows 3, 4 and 5.

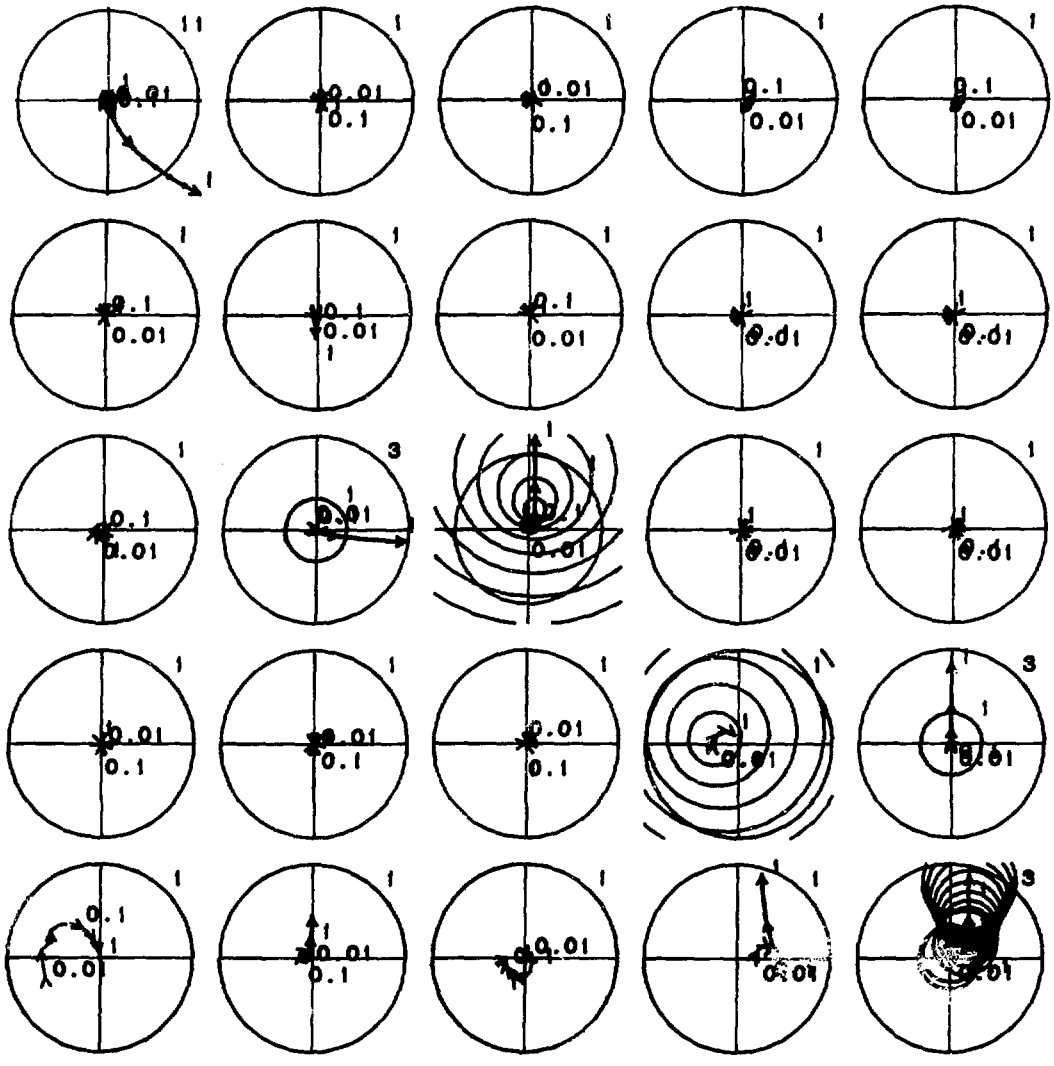

FIGURE 4.2 INA PLOT, GERSHGORIN CIRCLES - NO COMPENSATORS

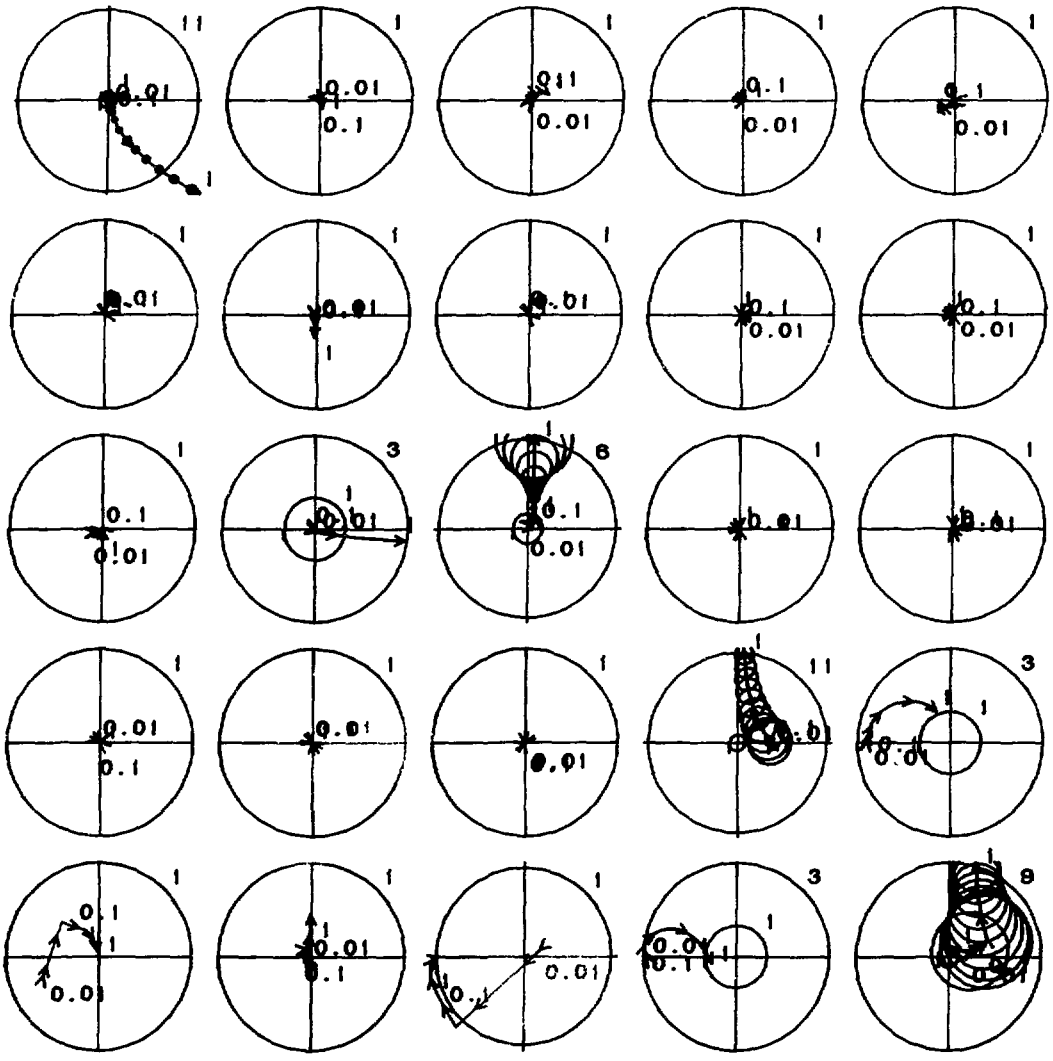

FIGURE 4.3 INA PLOT, GERSHGORIN CIRCLES - SEQUENCE 1

Operations performed:

```
COL A,5,4,-3
COL P,4,5
COL S,3,5
COL S,4,5
COL S,5,10
```

Results: row 3 and row 4 become dominant and row 5 is dominant for high frequencies, as shown in Figure 4.3 and Table 3.

TABLE 3

SEQUENCE 1: DOMINANCE RATIOS

ROW	DOM RATIO	FREQUENCY	NB FREQ
1	0.72	0.010	0
2	0.76	0.062	0
3	0.46	1.00	0
4	0.69	0.166	0
5	1.8	0.010	5

Sequence 2

Objectives: improve dominance of row 5 and amplify the Gershgorin band on row 2.

Operations performed:

```
COL S,1,0.9
COL S,3,0.51
COL S,4,1.02
COL S,5.1.45
```

Results: dominance of row 5 is still not achieved, as shown in Figure 4.4 and Table 4.

TABLE 4

SEQUENCE 2: DOMINANCE RATIOS

ROW	DOM RATIO	FREQUENCY	NB FREQ
1	0.94	0.010	0
2	0.66	0.062	0
3	0.91	1.00	0
4	0.98	0.166	0
5	1.2	0.010	1

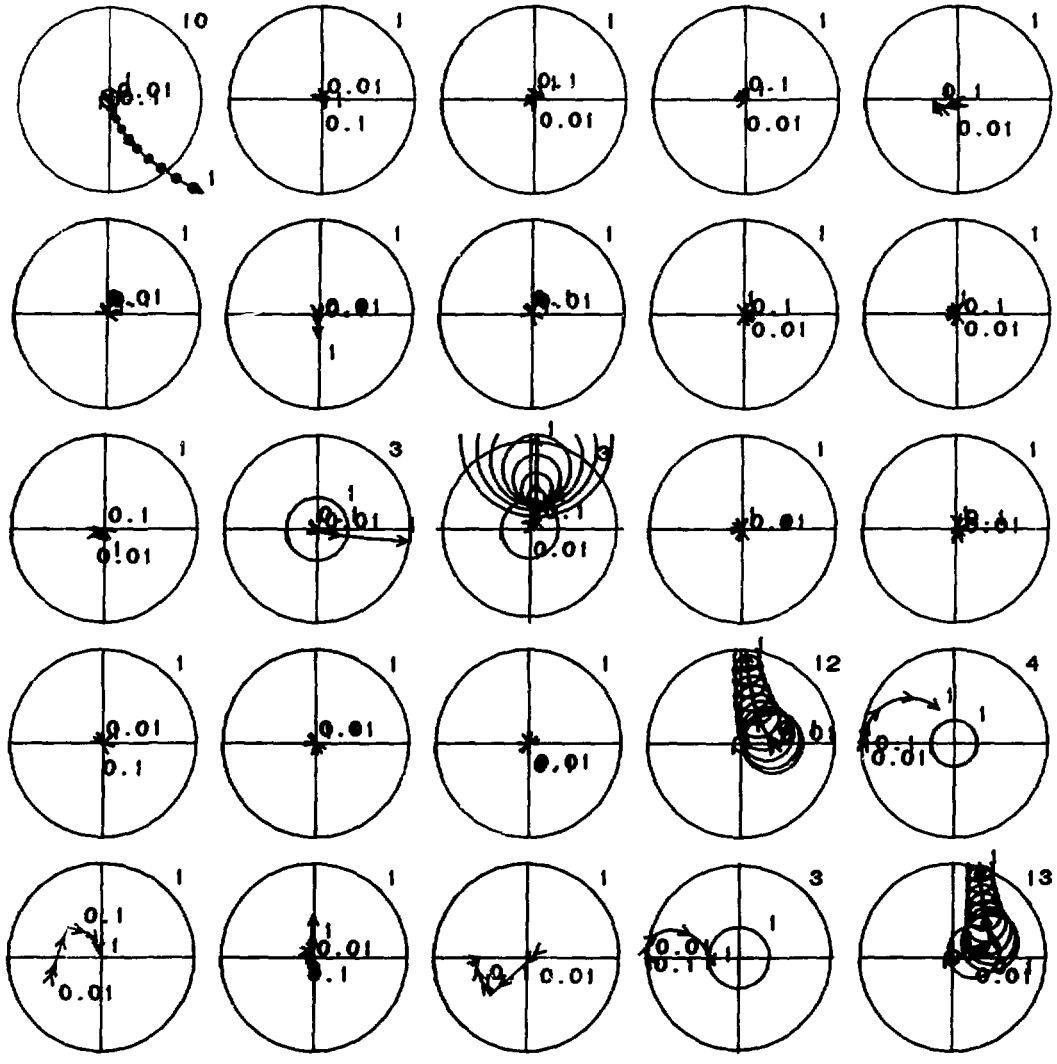

FIGURE 4.4 INA PLOT, GERSHGORIN CIRCLES - SEQUENCE 2

Sequence 3

Objectives: achieving dominance of row 5.

Operations performed:

```
ROW C,1
ROW C,4
COL S,1,0.3
ROW C,5
ROW C,3
ROW C,2
ROW C,4
ROW C,1
```

Results: row 5 is dominant, and dominance has been improved on the other rows as shown in Figure 4.5 and Table 5.

Note that the hillclimb algorithm was applied for 6 frequencies covering the frequency band.

TABLE 5

SEQUENCE 3: DOMINANCE RATIOS

ROW	DOM RATIO	FREQUENCY	NB FREQ
1	0.50	0.062	0
2	0.45	0.166	0
3	0.91	1.00	0
4	0.96	0.218	0
5	0.65	1.00	0

Sequence 4

Objectives: improve the dominance ratio on each row and amplify row 2.

Operations performed:

```
COL S,3,1.5
COL S,4,1.5
ROW C,5
COL S,5,1.3
ROW S,2,3
```

Results: the dominance ratios are improved, as shown in Figure 4.6 and Table 6.

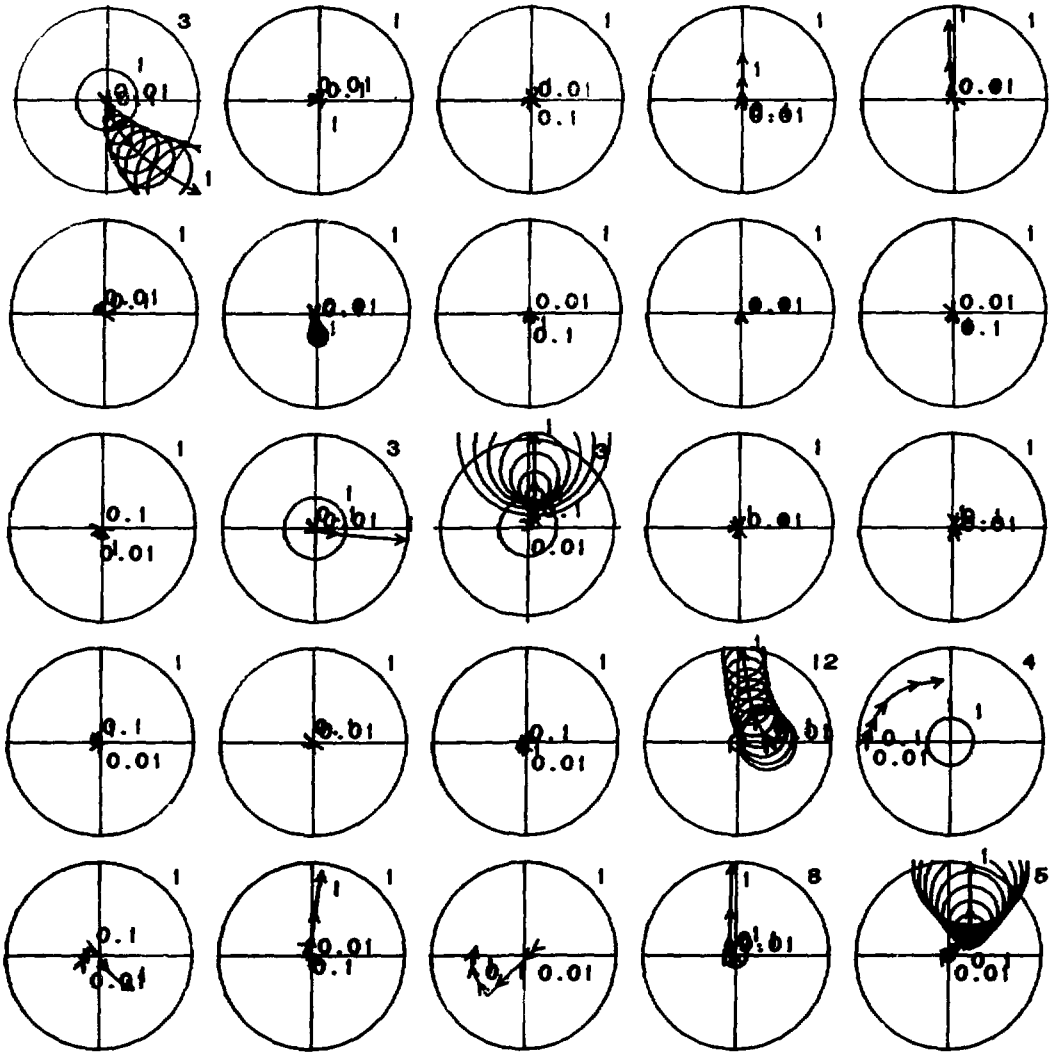

FIGURE 4.5 INA PLOT, GERSHGORIN CIRCLES - SEQUENCE 3

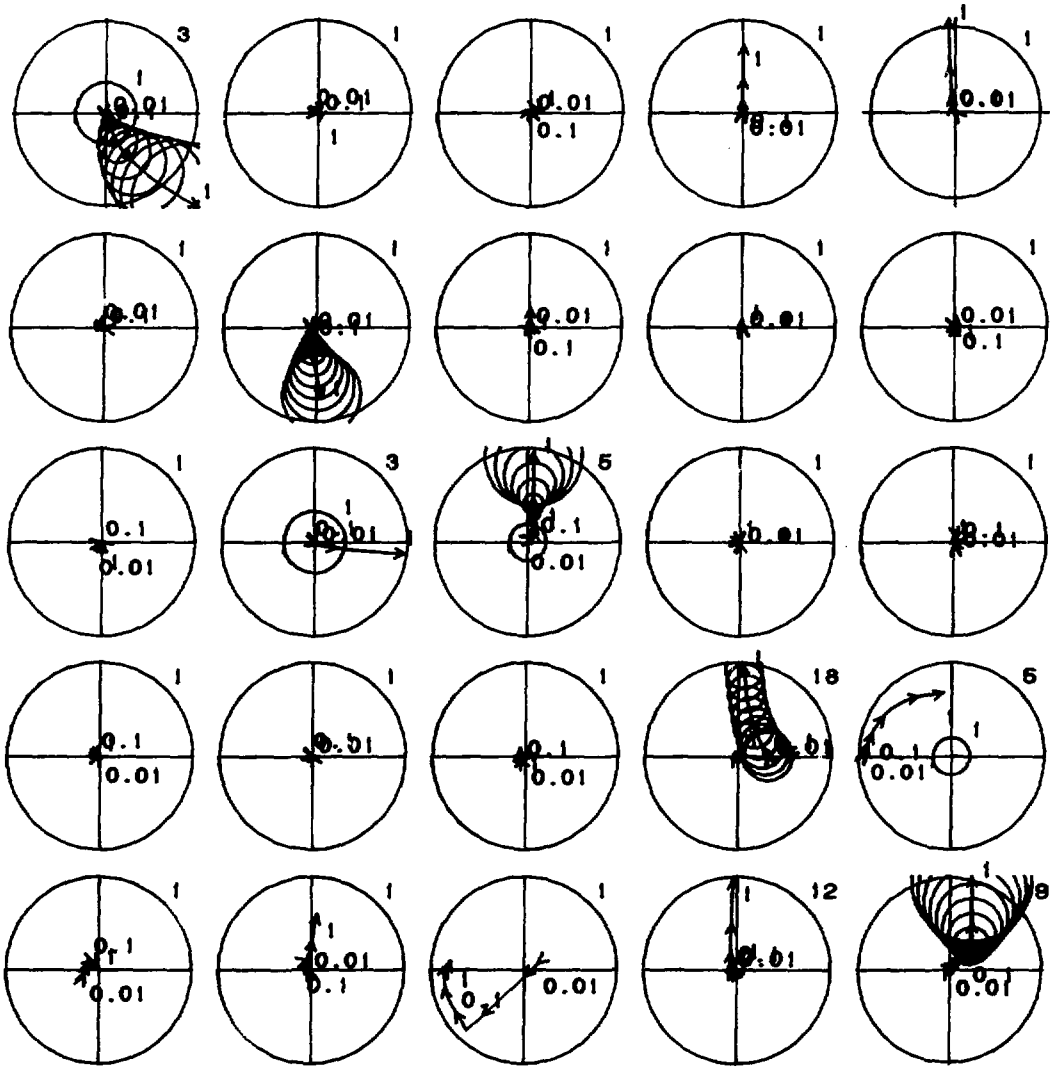

FIGURE 4.6 INA PLOT, GERSHGORIN CIRCLES - SEQUENCE 4

TABLE 6

SEQUENCE 4: DOMINANCE RATIOS

ROW	DOM RATIO
1	0.71
2	0.64
3	0.61
4	0.83
5	0.65

The compensator KI obtained in this sequence is a full matrix, because hill climbing has been applied to each row.

Sequence 5

Objectives: obtain comparable dominance ratios to previous results (Table 6), with a set of operations that will give a simpler compensator KI. The operations are applied to the matrix QI described in equation (21).

Operations performed:

```
COL A,5,4,-3
COL P,4,5
COL S,3,3
COL S,4,5
COL S,5,14
ROW C,1
COL S,1,0.3
ROW C,5
```

Results: dominance is achieved. The ratios obtained are shown in Table 7.

TABLE 7

SEQUENCE 5: DOMINANCE RATIOS

ROW	DOM RATIO
1	0.83
2	0.65
3	0.77
4	0.96
5	0.67

Sequence 6

Objectives: improve the dominance of rows 1 and 4.

Operations performed:

```
ROW C,1
COL S,4,1.2
COL S,5,1.1
ROW S,2,3
```

Results: the dominance is improved, as shown in Table 8. Comparison of Table 8 with Table 6 indicates that these two results are more or less equivalent.

TABLE 8

SEQUENCE 6: DOMINANCE RATIOS

ROW	DOM RATIO
1	0.62
2	0.69
3	0.77
4	0.88
5	0.70

4.3.3 Concluding Step

Now the dominance of the inverse transfer-function matrix QI(s) calculated in Sequences 5 and 6 is investigated over 100 points in the frequency band with the compensators obtained. Table 9 shows a dominance failure on row 2 for 2 frequencies.

TABLE 9

DOMINANCE RATIOS WITH 100 FREQUENCIES

ROW	DOM RATIO	FREQUENCY	NB FREQ
1	0.64	0.050	0
2	1.08	0.040	2
3	0.77	1.00	0
4	0.89	0.190	0
5	0.70	1.00	0

This result can be improved by applying the following operation:

```
ROW C,2
```

Results: dominance is completely achieved, as shown in Table 10.

TABLE 10

FINAL DOMINANCE RATIOS

ROW	DOM RATIO
1	0.64
2	0.75
3	0.77
4	0.89
5	0.70

Finally, the following operations are applied to scale rows 1, 2 and 4 by -1.

```
ROW S,1,-1
ROW S,2,-1
ROW S,4,-1
```

The diagonal of the matrix QI obtained is shown in Figure 4.7.

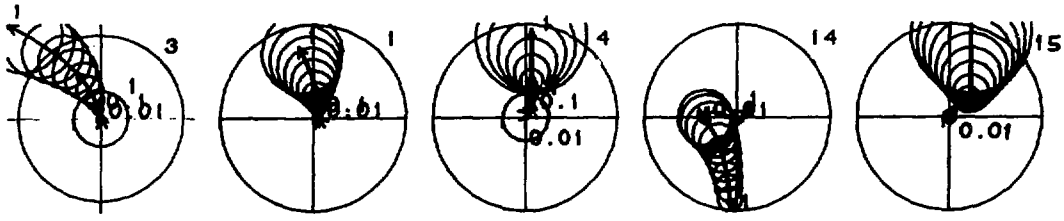

FIGURE 4.7 INA PLOT, GERSHGORIN CIRCLES
DIAGONAL ELEMENTS OF QI, FINAL CONFIGURATION

The final compensators LI and KI are inverted to give L and K, and now the system has the configuration shown in Figure 4.8.

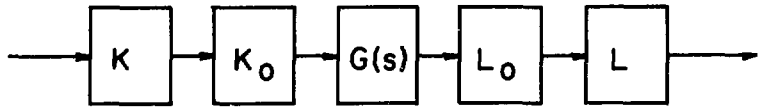

FIGURE 4.8 FINAL CONFIGURATION OF THE OPEN-LOOP SYSTEM

The matrices K and L obtained are:

$$K = \begin{bmatrix} -0.9994 & 4.115E-02 & -1.277E-02 & 2.469E-03 & -5.835E-02 \\ 3.502E-04 & -0.3333 & -1.875E-02 & 2.219E-04 & -2.132E-04 \\ 0.0000 & 0.0000 & 1.000 & 0.0000 & 0.0000 \\ 0.0000 & 0.0000 & 0.0000 & -1.000 & 0.0000 \\ -1.223E-02 & -0.5835 & 0.1501 & 0.6431 & 0.9995 \end{bmatrix}$$

and

$$L = \begin{bmatrix} 3.333 & 0.0000 & 0.0000 & 0.0000 & 0.0000 \\ 0.0000 & 1.000 & 0.0000 & 0.0000 & 0.0000 \\ 0.0000 & 0.0000 & 0.3333 & 0.0000 & 0.0000 \\ 0.0000 & 0.0000 & 0.0000 & 0.0000 & 0.1667 \\ 0.0000 & 0.0000 & 0.0000 & 6.494E-02 & 0.1948 \end{bmatrix}$$

With these compensators, the closed-loop analysis with the choice of the feedback gains is performed.

4.4 Closed-Loop Stability Analysis

4.4.1 General

The closed-loop stability analysis is performed with the use of a static, diagonal feedback matrix, F = diag (f_1,f_2,f_3,f_4,f_5).

The Gershgorin circles of Figure 4.7 indicate that the system will be stabilized with a positive gain f for loops 1, 2, 3 and 5, and a gain f smaller than approximately 5 for loop 4.

In a preliminary analysis, the loops are closed one by one. At each step, the eigenvalues for the closed-loop system are calculated and the Ostrowski circles are drawn to analyze the stability margin of the loops. Then, the choice of the final gains is performed.

4.4.2 Preliminary Analysis

First loop closed:

Ostrowski circles are shown in Table 11 for F = (4,0,0,0,0) with the corresponding closed-loop poles. The study of the system under various gains in the first loop indicates the following.

This loop does not have any effect on the unstable modes. However, fast modes are affected, and f_1 must be less than 2 to have acceptable damping on the fastest complex pair.

Ostrowski circles do not noticeably change in diameter when f_1 increases. The stability margin is thus insensitive to a variation of f_1, confirming the results of the modal analysis.

First and second loops closed:

Ostrowski circles are shown for F = (4,2,0,0,0) with the corresponding poles in Table 12. The study of the system under various gains for loop 2 indicates the following.

The second loop has stabilized one of the unstable modes. The value of the gain in this loop is mainly limited by the dynamic response of the turbine now associated with the fastest mode.

Ostrowski circles do not noticeably change in diameter. Increasing f_2 does not noticeably influence the stability margin of the system.

First three loops closed:

Ostrowski circles are shown for F = (4,4,4,0,0) with the corresponding eigenvalues in Table 13. The study of the system under various gains for loop 3 indicates the following.

The system has again two unstable modes and the turbine mode becomes faster. This is an indication of a strong interaction between loops 2 and 3. The other poles move only slightly.

Ostrowski circles shrink on loop 5, indicating a strong interaction between loops 3 and 5. The stability margin in loop 5 could be improved with a high f_3, but the value of f_3 is limited by the time constant of the fastest mode.

First four loops closed:

The Ostrowski circles are shown for F=(4,4,4,-4,0) with the corresponding poles in Table 14. The study of the system under various gains for loop 4 indicates the following.

TABLE 11

FIRST LOOP CLOSED

OSTROWSKI CIRCLES AND CLOSED-LOOP POLES

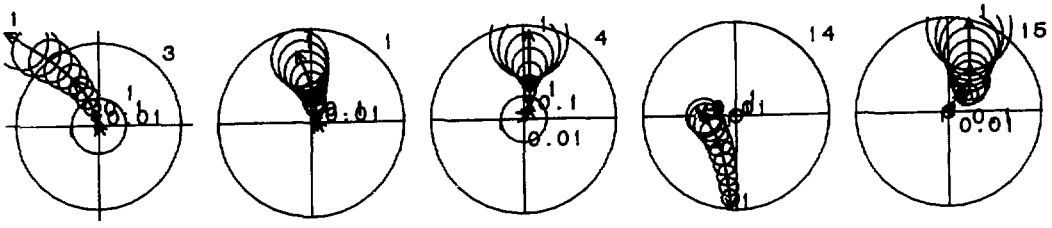

Mode No.	Real Value	Imaginary Value
1	1.243692E-07	0.000000
2	5.412651E-09	0.000000
3	0.000000	0.000000
4	-4.727954E-03	0.000000
5	-1.183942E-02	0.000000
6	-2.633332E-02	0.000000
7	-4.330219E-02	1.270701E-02
8	-4.330219E-02	-1.270701E-02
9	-0.127091	0.000000
10	-0.134717	0.291740
11	-0.134717	-0.291740
12	-0.180224	1.026394E-02
13	-0.180224	-1.026394E-02
14	-0.360324	0.000000
15	-0.429277	0.000000
16	-0.454545	0.000000
17	-0.500000	0.000000
18	-1.07955	0.000000
19	-1.81456	-2.59980
20	-1.81456	2.59980
21	-2.58547	0.000000
22	-2.79481	0.000000
23	-3.22072	-6.04003
24	-3.22072	6.04003

TABLE 12

FIRST AND SECOND LOOPS CLOSED

OSTROWSKI CIRCLES AND CLOSED-LOOP POLES

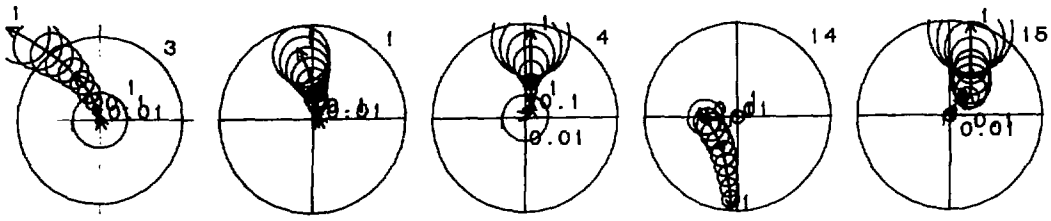

Mode No.	Real Value	Imaginary Value
1	0.000000	0.000000
2	-4.216723E-08	0.000000
3	-4.859866E-05	0.000000
4	-4.727954E-03	0.000000
5	-1.153231E-02	0.000000
6	-2.633335E-02	0.000000
7	-4.232238E-02	1.061136E-02
8	-4.232238E-02	-1.061136E-02
9	-0.127155	0.000000
10	-0.129503	0.279371
11	-0.129503	-0.279371
12	-0.177399	8.654718E-03
13	-0.177399	-8.654718E-03
14	-0.356512	0.000000
15	-0.429280	0.000000
16	-0.500000	0.000000
17	-1.07885	0.000000
18	-1.81461	-2.59984
19	-1.81461	2.59984
20	-2.58541	0.000000
21	-2.79493	0.000000
22	-3.22071	6.03980
23	-3.22071	-6.03980
24	-17.5704	0.000000

TABLE 13

FIRST THREE LOOPS CLOSED

OSTROWSKI CIRCLES AND CLOSED-LOOP POLES

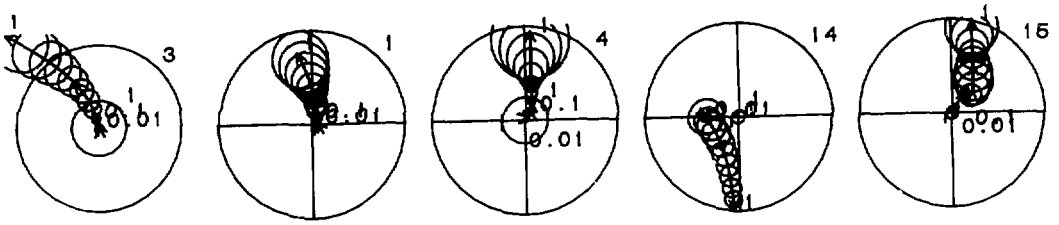

Mode No.	Real Value	Imaginary Value
1	7.226136E-05	0.000000
2	0.000000	0.000000
3	-4.727954E-03	0.000000
4	-1.438797E-02	0.000000
5	-2.633327E-02	0.000000
6	-4.703581E-02	1.228547E-02
7	-4.703581E-02	-1.228547E-02
8	-6.954551E-02	0.000000
9	-9.760229E-02	0.286669
10	-9.760229E-02	-0.286669
11	-0.112215	-2.138654E-02
12	-0.112215	-2.138654E-02
13	-0.173852	0.000000
14	-0.429349	0.000000
15	-0.499474	0.000000
16	-1.06952	0.000000
17	-1.81469	2.59982
18	-1.81469	-2.59982
19	-2.58547	0.000000
20	-2.79458	0.000000
21	-3.22057	6.03979
22	-3.22057	-6.03979
23	-4.85068	0.000000
24	-42.1457	0.000000

TABLE 14

FIRST FOUR LOOPS CLOSED

OSTROWSKI CIRCLES AND CLOSED-LOOP POLES

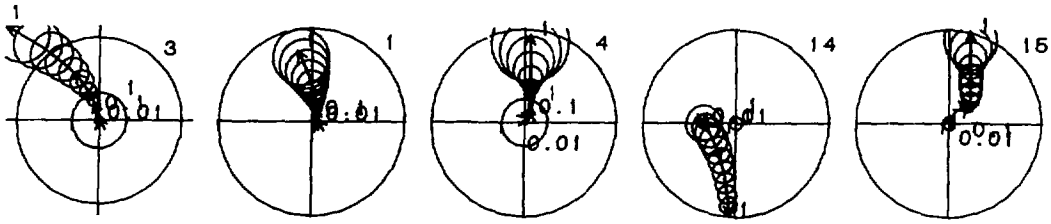

Mode No.	Real Value	Imaginary Value
1	1.558705E-09	0.000000
2	-4.727954E-03	0.000000
3	-7.623277E-03	0.000000
4	-1.444483E-02	0.000000
5	-2.633280E-02	0.000000
6	-4.741461E-02	1.217905E-02
7	-4.741461E-02	-1.217905E-02
8	-6.958628E-02	0.000000
9	-9.961549E-02	0.286408
10	-9.961549E-02	-0.286408
11	-0.113112	2.327464E-02
12	-0.113112	-2.327464E-02
13	-0.173845	0.000000
14	-0.429342	0.000000
15	-0.502302	0.000000
16	-1.31851	0.000000
17	-2.49057	-2.94200
18	-2.49057	2.94200
19	-2.57977	0.000000
20	-2.79598	0.000000
21	-3.22054	-6.03981
22	-3.22054	6.03981
23	-4.85068	0.000000
24	-42.1457	0.000000

Gain $f_4 > 0$ strongly destabilizes the system. With $f_4 < 0$, only one pole is unstable and its real value gets closer to zero when $|f_4|$ increases.

When f_4 increases from zero, the Ostrowski circles get much larger on loops other than 4 and the system loses its dominance (Ostrowski circles become larger than Gershgorin circles). The circles are smaller if f_4 is negative.

All loops closed:

Ostrowski circles are shown for F = (4,4,4,-4,4) with the corresponding poles in Table 15. The study of the system for various gains in loop 5 when the gain in loop 4 is negative indicates that a pole is still unstable when $f_5 > 0$, and its real value gets closer to zero when f_5 increases.

The Ostrowski circles shrink on loops other than 5 when f_5 varies between 0 and 4. Gain f_5 influences the location of the slowest mode and most of the other poles. Interaction between loop 5 and other loops is thus also very strong.

Now, the effect of a positive gain in loop 4 with loop 5 closed is studied. The Ostrowski circles are shown for F = (4,4,4,2,4) with the corresponding poles in Table 16. The system is stabilized. This result indicates that the influence of gain in loop 5 on stability margin in loop 4 is very strong. Also the Ostrowski circles get larger when f_4 varies between 0 and 2.

4.4.3 Choice of Gains

The results can be summarized as follows:

(1) To have a reasonable time constant for the fastest pole:

$$f_2 < 1.5$$

low gain on f_3.

(2) To have non-oscillatory poles #22-23:

$$f_1 < 2$$

(3) To speed up the slowest modes:

high gain on f_4

low f_5, but >0.1 to preserve stability.

(4) To decrease oscillatory nature of poles 9-10 (10-11 in open loop):

high gain on f_1

$$f_3 < 2$$

TABLE 15

ALL LOOPS CLOSED, $f_4 < 0$

OSTROWSKI CIRCLES AND CLOSED-LOOP POLES

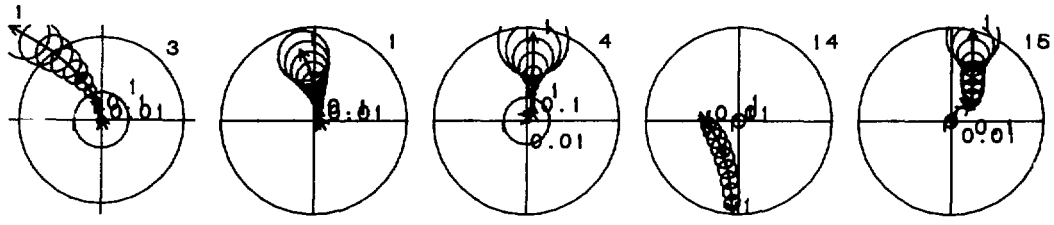

Mode No.	Real Value	Imaginary Value
1	4.812978E-11	0.000000
2	-4.727954E-03	0.000000
3	-1.433109E-02	0.000000
4	-2.633337E-02	0.000000
5	-4.478226E-02	1.161508E-02
6	-4.478226E-02	-1.161508E-02
7	-6.897139E-02	0.000000
8	-8.420918E-02	0.000000
9	-9.490327E-02	0.271946
10	-9.490327E-02	-0.271946
11	-0.138785	0.000000
12	-0.174422	0.000000
13	-0.195675	0.000000
14	-0.429339	0.000000
15	-0.514349	0.000000
16	-2.25889	0.000000
17	-2.43482	0.000000
18	-2.82866	0.000000
19	-2.83718	2.83109
20	-2.83718	-2.83109
21	-3.21955	-6.03990
22	-3.21955	6.03990
23	-4.85074	0.000000
24	-42.1457	0.000000

TABLE 16

ALL LOOPS CLOSED, $f_4 > 0$

OSTROWSKI CIRCLES AND CLOSED-LOOP POLES

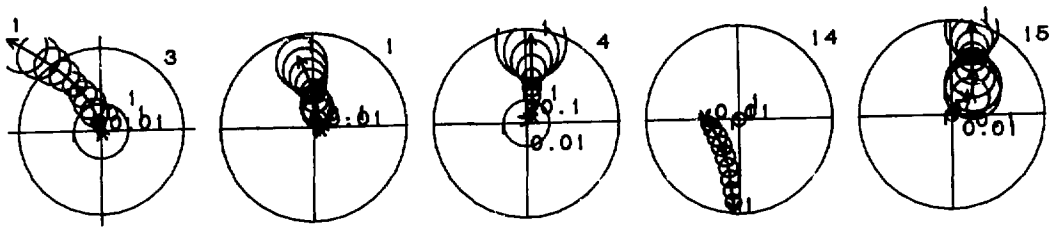

Mode No.	Real Value	Imaginary Value
1	-8.206170E-11	0.000000
2	-4.727954E-03	0.000000
3	-1.433084E-02	0.000000
4	-2.633324E-02	0.000000
5	-4.478787E-02	1.161687E-02
6	-4.478787E-02	-1.161687E-02
7	-6.896613E-02	0.000000
8	-8.406587E-02	0.000000
9	-9.412470E-02	0.272810
10	-9.412470E-02	-0.272810
11	-0.140315	0.000000
12	-0.174791	0.000000
13	-0.186297	0.000000
14	-0.429353	0.000000
15	-0.511155	0.000000
16	-1.36539	0.000000
17	-2.03580	1.91863
18	-2.03580	-1.91863
19	-2.52926	0.000000
20	-2.82236	0.000000
21	-3.21961	-6.03983
22	-3.21961	6.03983
23	-4.85075	0.000000
24	-42.1457	0.000000

(5) To keep small Ostrowski circles:

high gain on f_3 and f_5

$f_4 < 2$

The feedback matrix F = diag(1.2,1,0.5,1.7,0.3) has been found to be satisfactory. For this F, the poles are shown in Table 17 with the Ostrowski circles. The simulation of the system with this feedback matrix is performed to fine tune the gains if the closed-loop system response is not satisfactory.

4.4.4 Simulation of the Closed-Loop System

To simulate the system using module MVSIM, the configuration of the closed-loop system must be modified as shown in Figure 4.9.

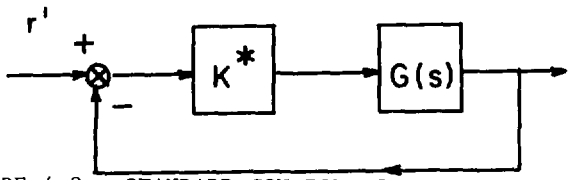

FIGURE 4.9 STANDARD CONFIGURATION OF THE CONTROL SYSTEM

where the controller matrix

$$K^* = K_o \cdot K \cdot F \cdot L \cdot L_o \qquad (22)$$

has the structure shown in Table 18.

This configuration enables the controller to respond to measurements of plant output deviations.

Figures 4.10 (a) and (b) show the closed-loop response of the design model to a 1% decrease in reactor and turbine power setpoints. The results are in general satisfactory. The system is stable and has some fast dynamics, especially the reactor power. The reactor and the turbine powers show perfect steady-state performance. The initial transients in the reactor power and the steam generator pressure can be improved by fine tuning the gains in the associated loops. The steady-state offsets on the steam generator pressure and level can also be reduced by addition of integral actions. However, experience [2] has shown that fine tuning of controllers with a linear model does not guarantee improved performance on the reference non-linear model. In this study, any required fine tuning is performed directly on G2SIM to take into account the non-linearities.

TABLE 17

CHOICE OF GAINS FOR SIMULATION

OSTROWSKI CIRCLES AND CLOSED-LOOP POLES

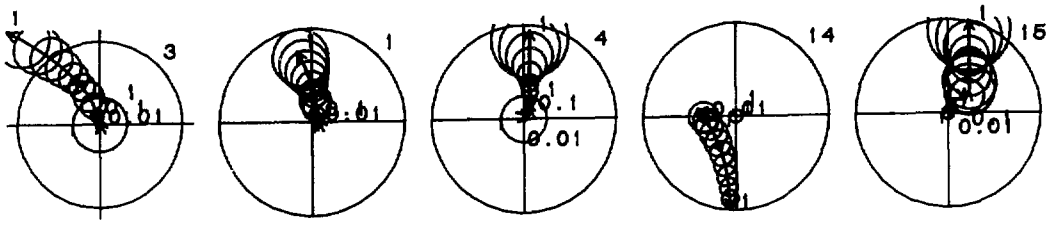

Mode No.	Real Value	Imaginary Value
1	-1.682941E-09	0.000000
2	-4.730965E-03	0.000000
3	-8.434443E-03	0.000000
4	-1.490263E-02	0.000000
5	-2.632797E-02	0.000000
6	-4.310931E-02	1.715665E-02
7	-4.310931E-02	-1.715665E-02
8	-4.464365E-02	0.000000
9	-0.104370	0.279028
10	-0.104370	-0.279028
11	-0.126993	1.794114E-02
12	-0.126993	-1.794114E-02
13	-0.168685	0.000000
14	-0.475814	0.000000
15	-0.495410	0.000000
16	-0.888823	0.000000
17	-1.22446	0.000000
18	-1.60958	-2.34205
19	-1.60958	2.34205
20	-2.58315	0.000000
21	-2.76780	-0.000000
22	-3.21938	-1.66001
23	-3.21938	1.66001
24	-9.29128	0.000000

TABLE 18

CONTROLLER MATRIX DERIVED WITH THE INA METHOD

$$K^* = \begin{bmatrix} -39.97 & -1.137E\text{-}02 & -2.710E\text{-}02 & -2.129E\text{-}02 & 0.4115 & 2.129E\text{-}02 & -2.057 & 1.137E\text{-}02 \\ 0.0000 & 0.0000 & -2833. & 0.0000 & 0.0000 & 0.0000 & 0.0000 & 0.0000 \\ -0.4893 & 0.1947 & 2.406 & 0.2501 & -5.835 & -0.2501 & 29.18 & -0.1947 \\ 0.0000 & 0.0000 & 0.0000 & 1.667 & 0.0000 & -1.667 & 0.0000 & 0.0000 \\ 1.401E\text{-}02 & -4.153E\text{-}05 & 5.041E\text{-}04 & -3.125E\text{-}02 & -3.333 & 3.125E\text{-}02 & 16.67 & 4.153E\text{-}05 \end{bmatrix}$$

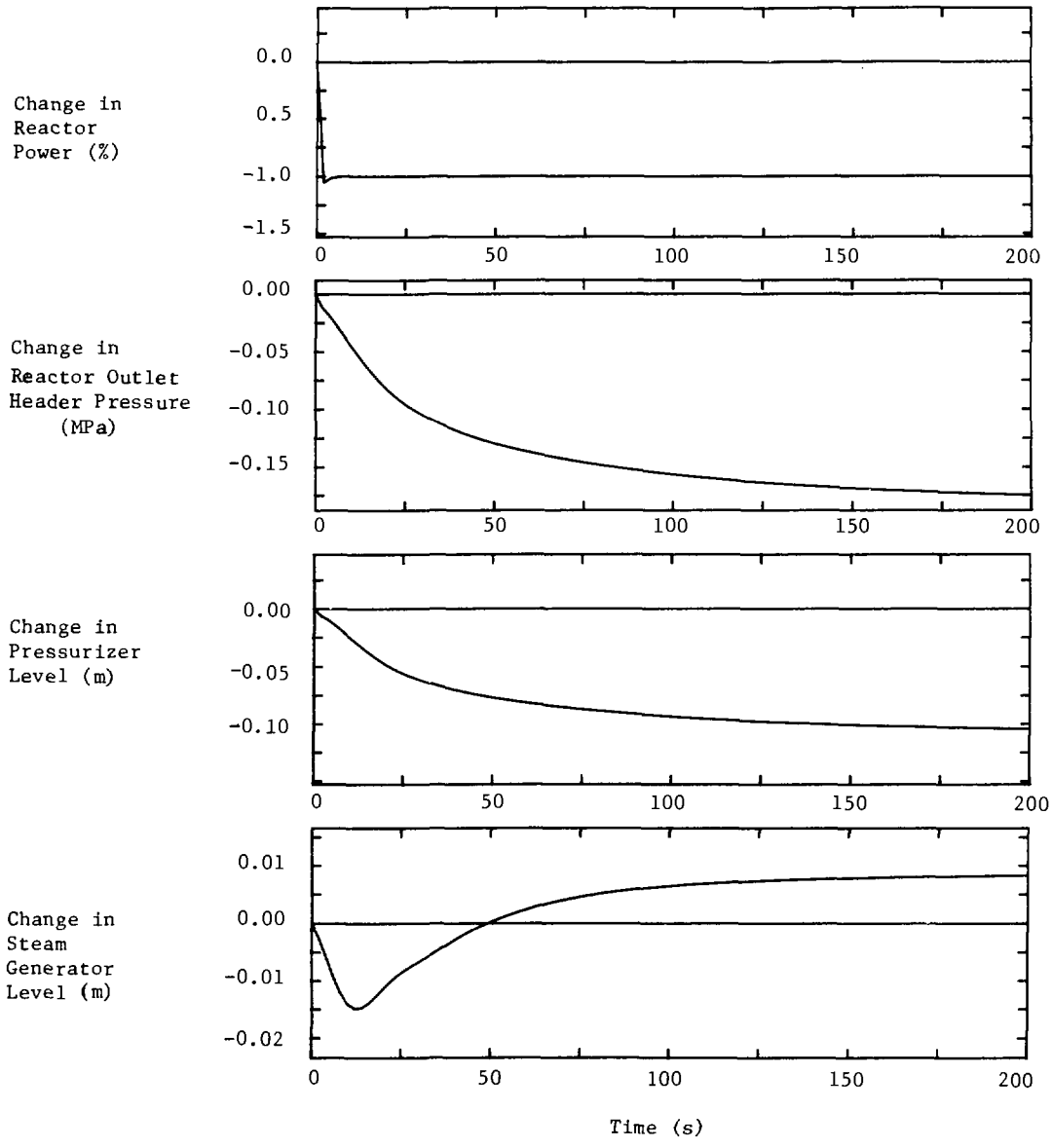

FIGURE 4.10(a) CLOSED-LOOP RESPONSE OF THE DESIGN MODEL TO 1% REDUCTION IN REACTOR AND TURBINE POWER SETPOINTS

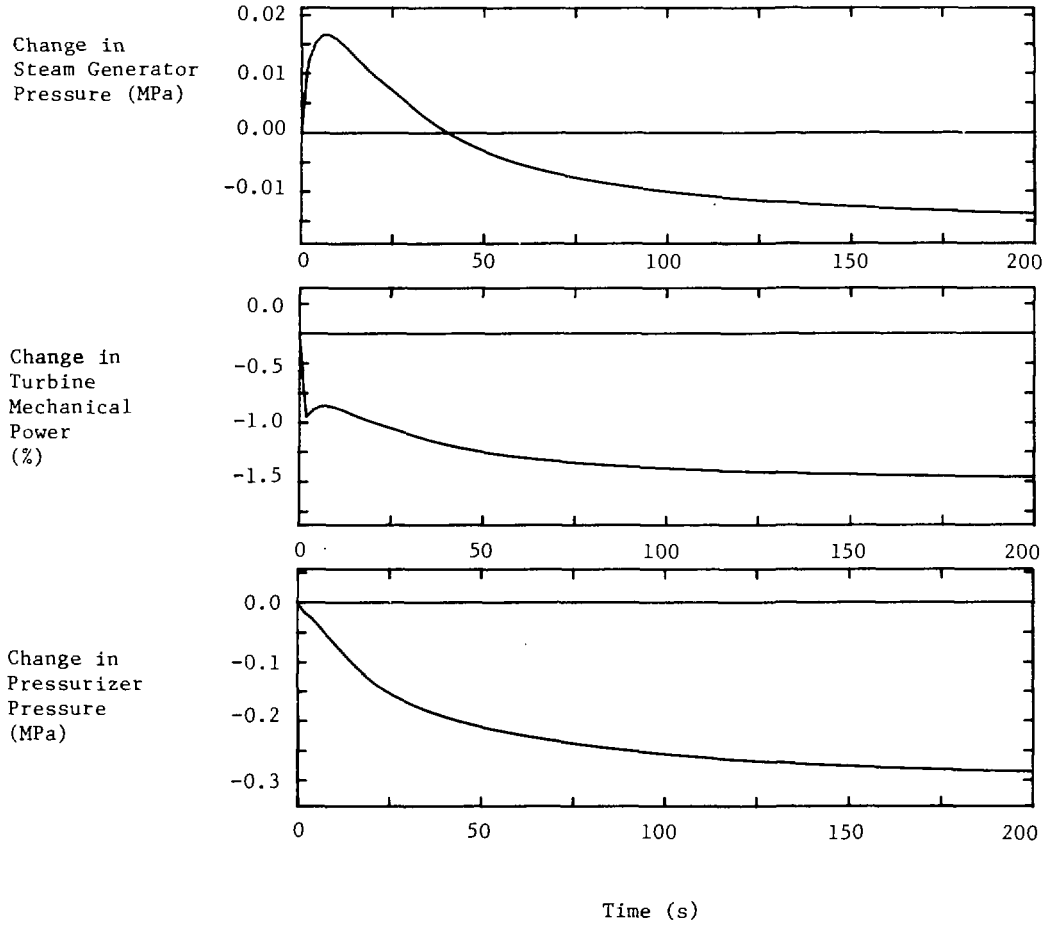

FIGURE 4.10(b) CLOSED-LOOP RESPONSE OF THE DESIGN MODEL TO 1% REDUCTION IN REACTOR AND TURBINE POWER SETPOINTS

5. IMPLEMENTATION AND PERFORMANCE ON G2SIM

5.1 Introduction

In this chapter, the implementation of the controller on the non-linear model G2SIM is described. Then simulation analysis is performed and the overall performance of the controller is studied. Integral actions are added to the control loops of the reactor power, the steam generator pressure and the steam generator level to improve the steady state tracking capability of the controller.

5.2 Implementation on G2SIM

The G2SIM program used in this study has the capability to incorporate conventional or multivariable controllers [2]. For the closed-loop simulation of G2SIM with a multivariable controller, the input vector actually applied at the sampling time kT is given by [2]

$$u_k = u_{k-1} + \Delta u_k \tag{23}$$

$$\Delta u_k = C_c \Delta \alpha_k + D_c \Delta e_k \tag{24}$$

where $\Delta\alpha_k$, the incremental state vector of the controller, is given by

$$\Delta \alpha_k = A_c \alpha_{k-1} + B_c e_{k-1} \tag{25}$$

and Δe_k, the incremental deviation error, is given by

$$\Delta e_k = \Delta(y-r')_k \tag{26}$$

Because the controller calculated in Section 4 is a pure proportional regulator, matrices A_c, B_c and C_c are null matrices while matrix D_c is given by

$$D_c = -K^* \tag{27}$$

5.3 Performance of Multivariable Controller on G2SIM

Simulation techniques are used to study the performance of the INA controller on G2SIM. In Figures 5.1(a,b), the response of the INA controller to a 1% reduction in reactor and turbine power setpoints is compared to the response of the conventional controller. These results show that after 200 seconds, the system is stable, and the overshoots are small. Except for the steady-state offsets, the overall performance of both controllers is very comparable.

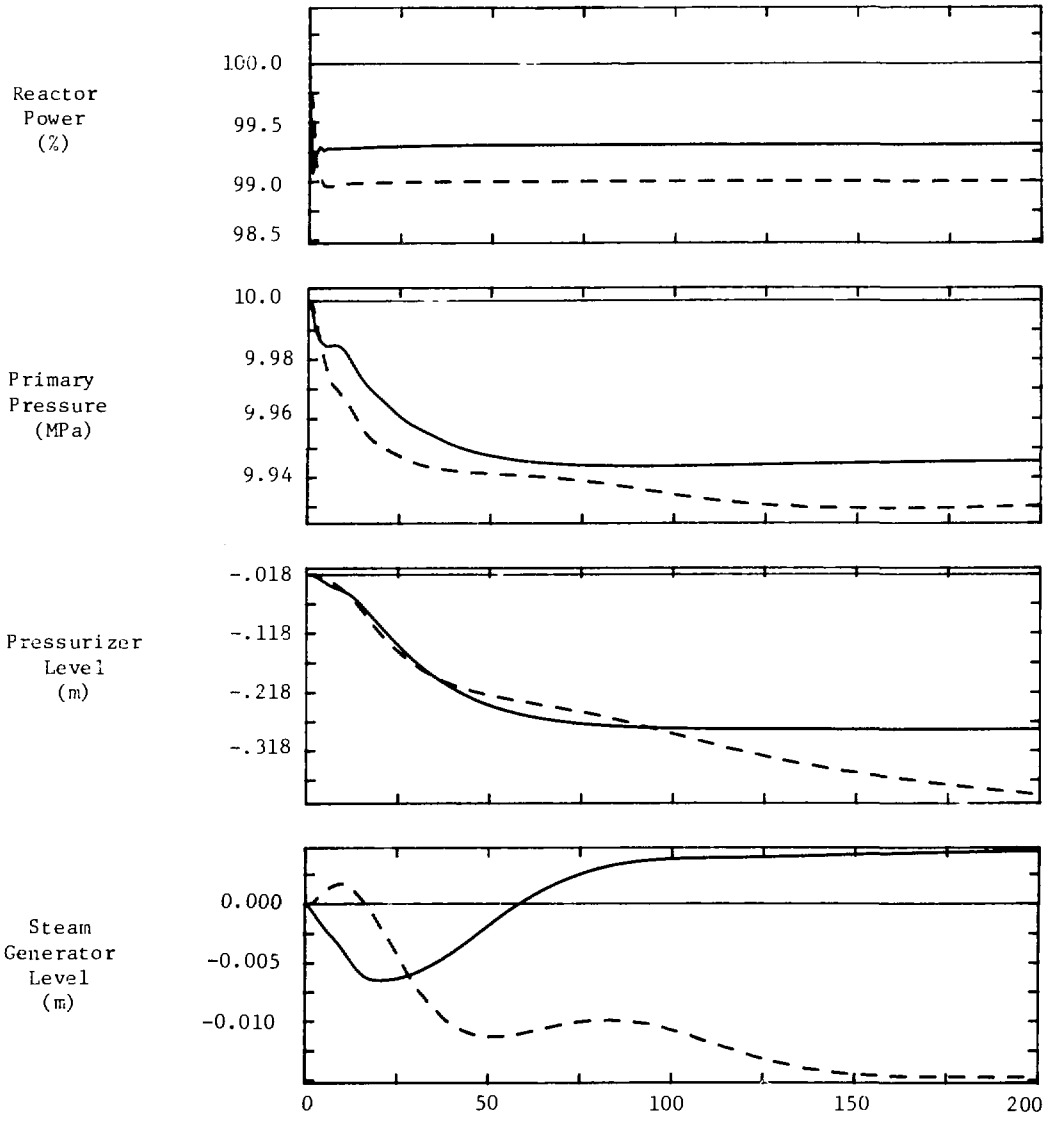

FIGURE 5.1(a) RESPONSE OF G2SIM TO 1% REDUCTION IN REACTOR AND TURBINE POWER SETPOINTS, FOR THE MULTIVARIABLE CONTROLLER AND THE CONVENTIONAL CONTROLLER

———— multivariable controller

– – – – – – – – – – conventional controller

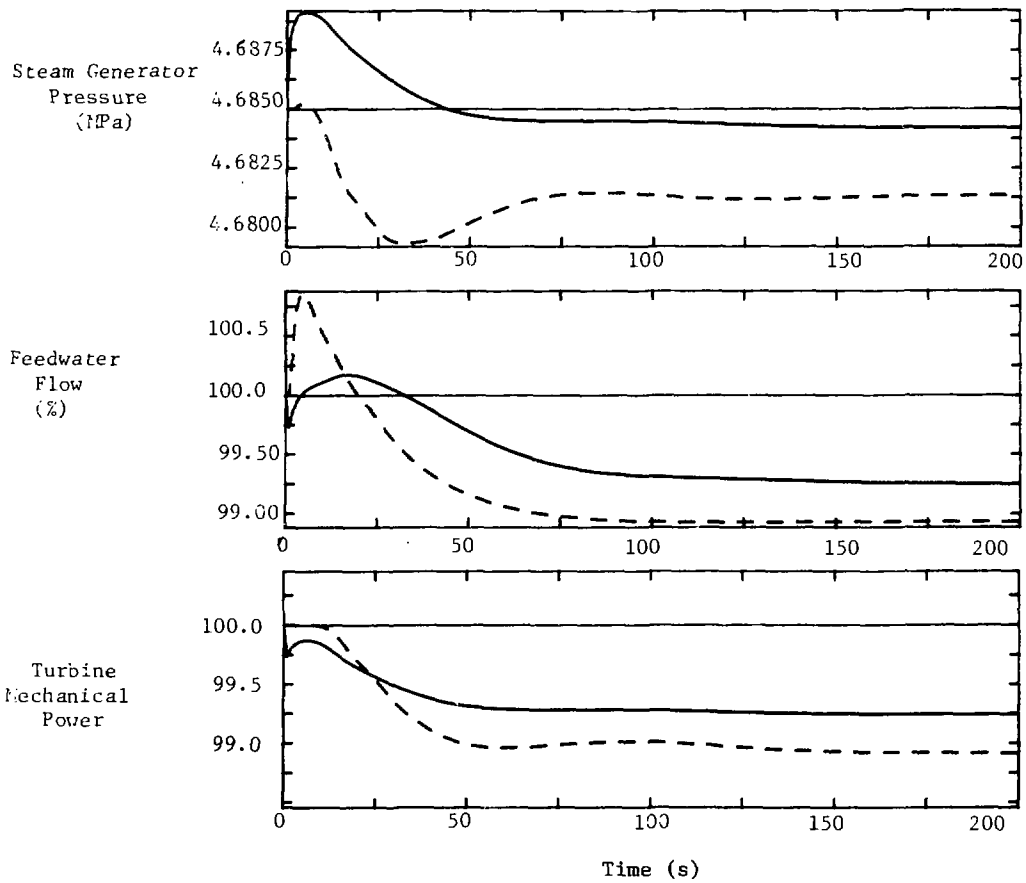

FIGURE 5.1(b) RESPONSE OF G2SIM TO 1% REDUCTION IN REACTOR AND TURBINE POWER SETPOINTS, FOR THE MULTIVARIABLE CONTROLLER AND THE CONVENTIONAL CONTROLLER

_____ multivariable controller

---------- conventional controller

Now although the multivariable controller has been designed for small signal perturbations, its robustness under large signal transients should be analyzed. Figures 5.2(a,b) show the response of G2SIM to a 5% reduction in the reactor and the turbine power setpoints. The results indicate that the system is stable and the overshoots are small, but the steady-state performance of the proportional multivariable controller is totally unacceptable. To eliminate this deficiency, the action of an integral controller has been investigated.

5.4 Addition of Integral Controller

After analyzing the steady-state performance of the multivariable controller, it was decided to add integral actions to the control loops of the reactor power, the steam generator level and the steam drum pressure. The gains of the integral controller were selected via manual tuning. The resulting controller is a multivariable-proportional-integral controller which can be described by equations (23) to (26), where A_c is a null matrix, and matrices B_c, C_c and D_c are

$$B_c = \begin{bmatrix} 0.5 & 0 & 0 & 0 & 0 & 0 & 0 & 0 \\ 0 & 0 & 0 & 0.3 & 0 & 0 & 0 & 0 \\ 0 & 0 & 0 & 0 & 0.1 & 0 & 0 & 0 \end{bmatrix}$$

$$C_c = \begin{bmatrix} 0.5 & 0 & 0 \\ 0 & 0 & 0 \\ 0 & 0 & 0 \\ 0 & -0.007 & 0 \\ 0 & 0 & 0.1 \end{bmatrix} \qquad D_c = -K^*$$

The response of the resulting closed-loop system to a 5% reduction in the reactor and the turbine power setpoints is shown in Figures 5.2(a,b). This figure indicates that the introduction of the integral action has eliminated completely the steady-state offsets on the reactor and the turbine power, and on the pressure and the level of the steam generator.

Finally, Figure 5.3 presents a comparison between the multivariable controller with integral action and the conventional controller. Again, the perturbation applied is a 5% reduction of the reactor and the turbine power setpoints. The results show that

(1) the response of the reactor power is slightly slower but smoother with the multivariable controller,

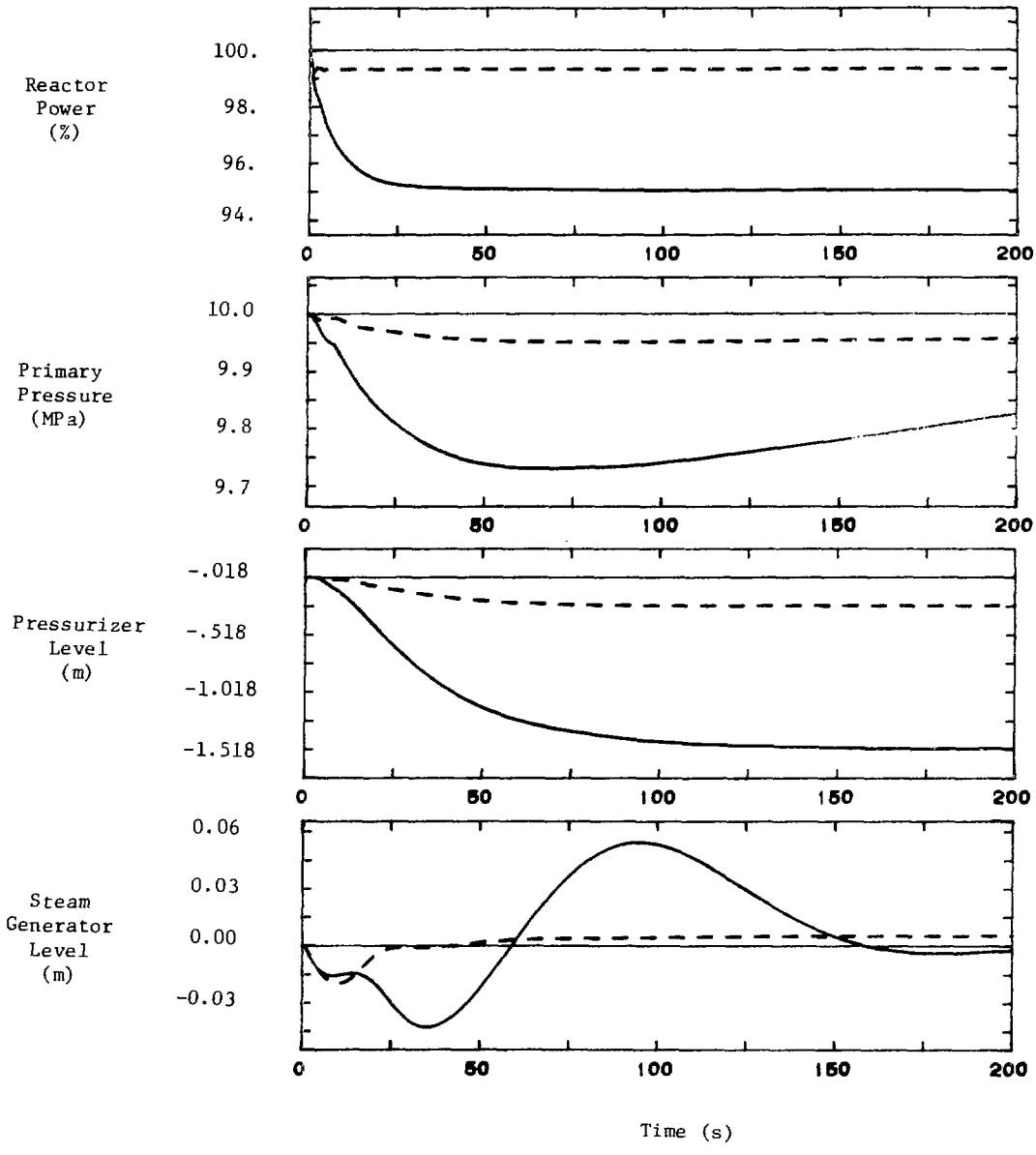

FIGURE 5.2(a) RESPONSE OF G2SIM to 5% REDUCTION IN THE REACTOR AND TURBINE POWER SETPOINTS, FOR THE MULTIVARIABLE CONTROLLER WIT' AND WITHOUT INTEGRAL CONTROL

———————— multivariable controller with integ' l action

- - - - - - - - - - - - multivariable controller without integral action

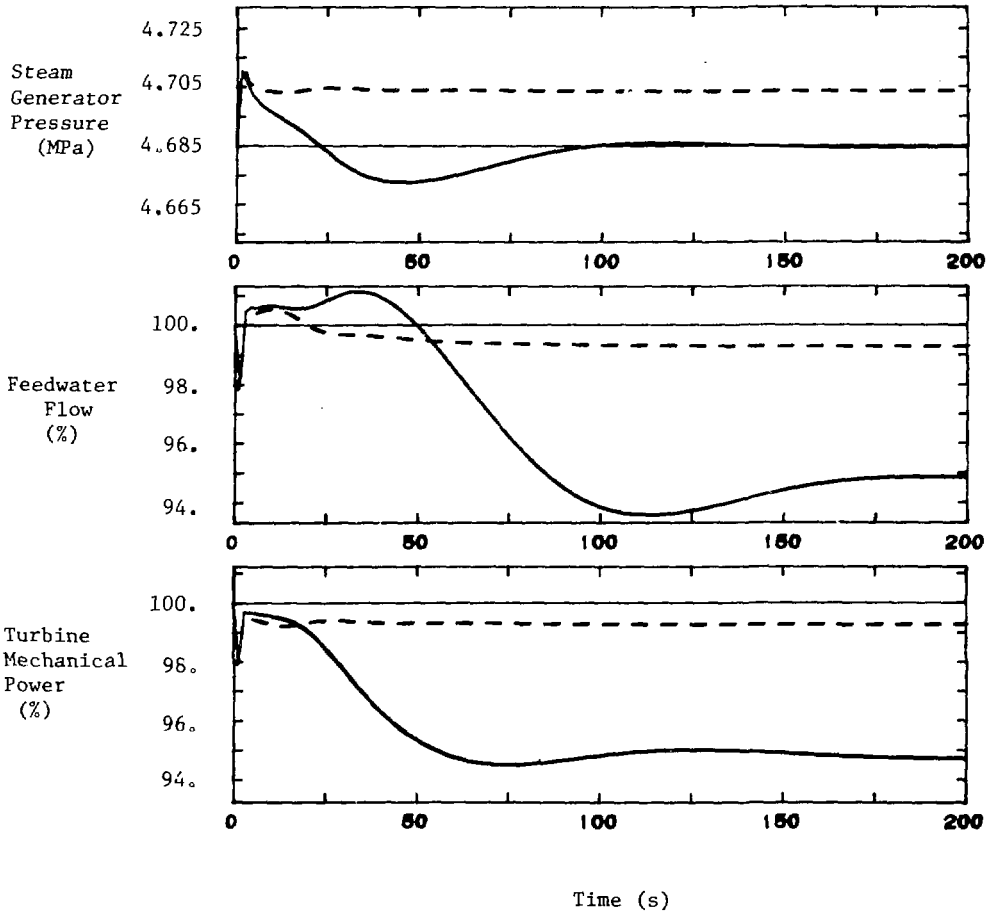

FIGURE 5.2(b) RESPONSE OF G2SIM TO 5% REDUCTION IN THE REACTOR AND TURBINE POWER SETPOINTS, FOR THE MULTIVARIABLE CONTROLLER WITH AND WITHOUT INTEGRAL CONTROL

———— multivariable controller with integral action

---------- multivariable controller without integral action

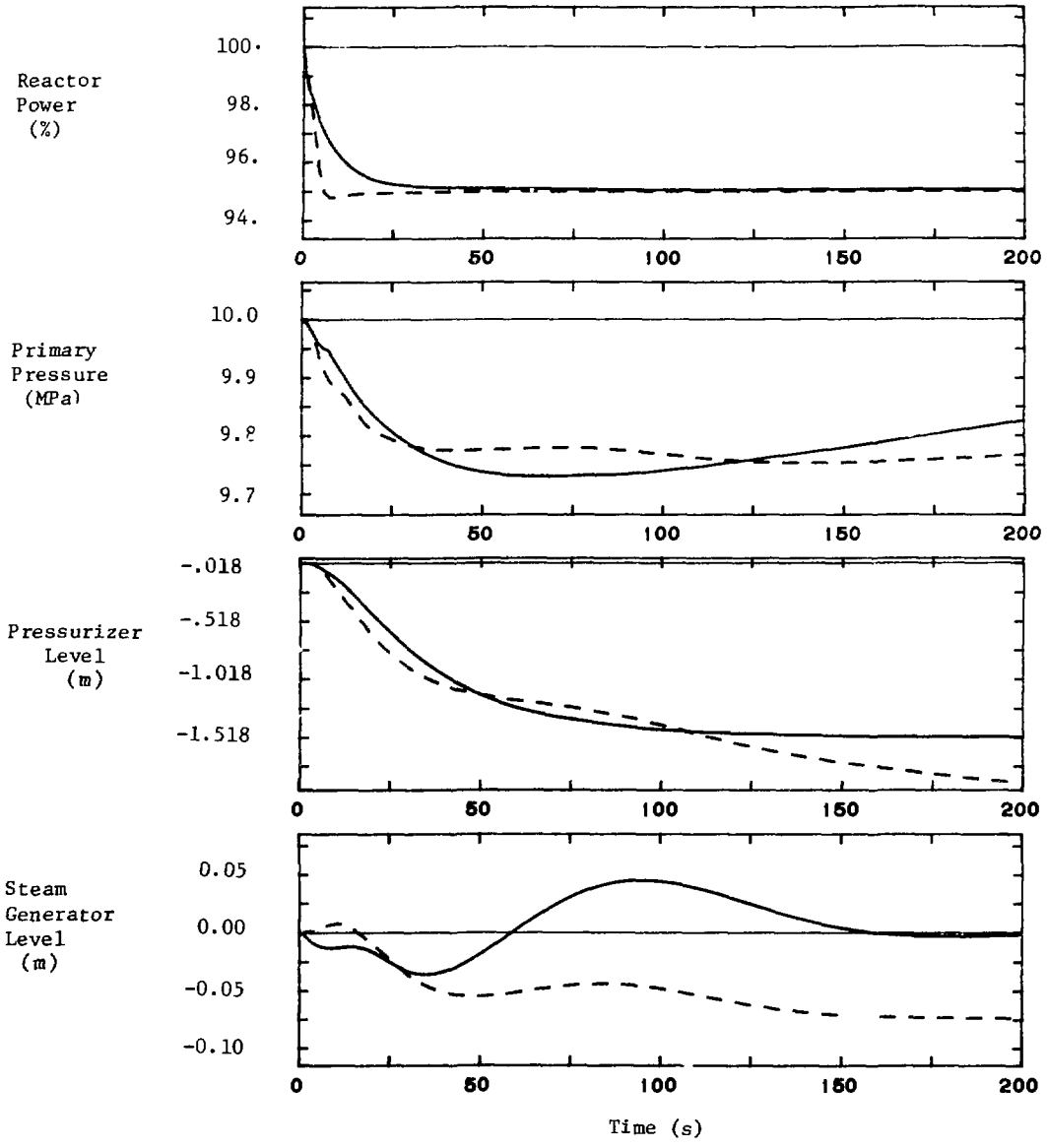

FIGURE 5.3(a) RESPONSE OF G2SIM TO 5% REDUCTION IN REACTOR AND TURBINE POWER SETPOINTS FOR THE MULTIVARIABLE CONTROLLER WITH INTEGRAL ACTION AND THE CONVENTIONAL CONTROLLER

———— multivariable controller with integral action

---------- conventional controller

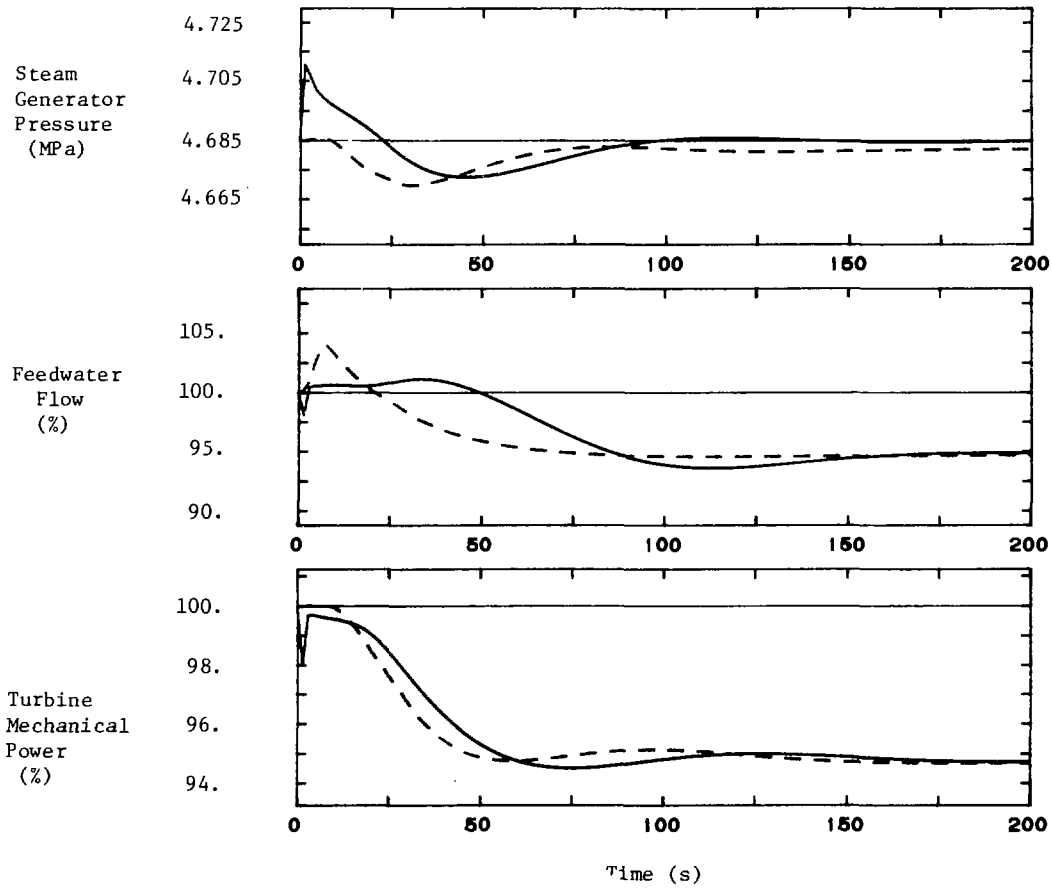

FIGURE 5.3(b) RESPONSE OF G2SIM TO 5% REDUCTION IN REACTOR AND TURBINE POWER SETPOINTS FOR THE MULTIVARIABLE CONTROLLER WITH INTEGRAL ACTION AND THE CONVENTIONAL CONTROLLER

_____ multivariable controller with integral action

---------- conventional controller

(2) the multivariable controller provides a more effective regulation on the primary pressure and on the pressurizer level,

(3) the response of the steam generator level shows a better steady-state performance with the multivariable controller,

(4) the response of the steam generator pressure shows an acceptable overshoot of 0.4% and perfect steady-state performance, and

(5) the response of the feedwater flow and the turbine power is very comparable for the two controllers.

In general, the results shown in Figures 5.3(a,b) indicate very well that a multivariable controller leads to an improved regulation of the plant in an overall sense.

6. CONCLUSIONS

In the study presented in this report, a multivariable controller has been designed for the regulation of a non-linear and complex model (G2SIM) of a CANDU 600 MWe nuclear reactor. In this study, the linear model (G2LDM) especially derived from G2SIM for control system analysis has been used as the plant design model. The state space description of G2LDM has been converted into a transfer-function representation to allow the design of the controller in the frequency domain. The well known Rosenbrock's Inverse Nyquist Array (INA) method has been used to study and achieve open-loop dominance.

After the open-loop dominance has been obtained, stability margins assessment through the inspection of Ostrowski circles, and analysis of modes distribution were used to select a proportional diagonal feedback matrix. As shown in Figures 4.10(a,b), the closed-loop response of the resulting proportional multivariable controller on the linear design model, G2LDM, is excellent.

Designed using a linear model, the actual performance of the multivariable controller must be assessed on the non-linear model. For this, the controller has been incorporated into the real-time simulation program of G2SIM. As shown in Figures 5.1(a,b), the performance of the proportional multivariable controller (without any tuning) on G2SIM are quite comparable to the conventional controller. However, the results shown in Figures 5.2(a,b) clearly indicate that under large perturbations, the steady-state tracking capability of the multivariable controller is unacceptable. Integral action was thus introduced in the control loops of the reactor power, the steam generator level, and the steam drum pressure to eliminate the undesirable steady-state offsets. The gains of the integral controller were adjusted during simulation tests. The results of Figure 5.3(a,b) show that when compared to the conventional controller, the resulting proportional integral multivariable controller achieves better overall regulation on G2SIM. This demonstrates that the INA method can be used successfully to design controllers for large and complex systems.

With the exception of the real-time non-linear simulations of G2SIM, the present study has been carried out completely within the framework provided by MVPACK. The underlying mathematical support and the extensive matrix manipulation required in this study illustrate well the capability available in MVPACK.

7. ACKNOWLEDGEMENTS

The technical support provided by the Dynamic Analysis Laboratory staff, especially G. Frketich and W.T. Howatt, is greatfully acknowledged. The contribution of Dr. P.D. McMorran in the definition and preliminary analysis of this project is also greatfully acknowledged. The project has received the unwavering support of our Branch Head, Dr. E.O. Moeck, and of Prof. A. Tapucu, Head of Institut de Genie Nucléaire, Ecole Polytechnique de Montreal.

8. REFERENCES

[1] P.D. McMorran, "Multivariable Control in Nuclear Power Stations, Survey of Design Methods", Atomic Energy of Canada Limited, AECL-6583, 1979 December.

[2] S. Mensah, "Contrôleur Multivariable pour une Centrale Nucléaire CANDU 600 MWe", Atomic Energy of Canada Limited, AECL-7841F, 1982 November.

[3] H.H. Rosenbrock, "Computer-Aided Control System Design", Academic Press, London, 1974.

[4] J.P. Lucas, Atomic Energy of Canada Limited, private communication.

[5] Wang Sin-Lin and Kai Ping-An, "Design of Diagonal Dominance by Compensators", Int. J. Control, Vol. 38, pp. 221-227, 1983.

[6] H.H. Rosenbrock, "An Automatic Method for Finding the Greatest or Least Value of a Function", The Computer Journal, Vol. 3, pp. 175-184, 1960.

[7] S. Mensah, "MVPACK: A Package for the Computer-Aided Design of Multivariable Control Systems", Atomic Energy of Canada Limited, AECL-8259, 1984.

[8] P.D. McMorran et al., Chalk River Nuclear Laboratories, private communication.

APPENDIX

DESCRIPTION OF THE LINEAR DESIGN MODEL

MATRIX A

1	-6.45233	4.726689E-03	0.415087	-7.436131E-03	0.000000	7.436131E-03	0.000000	0.000000
	7.75044	1107.21	0.000000	0.000000	0.000000	0.000000	0.000000	0.000000
	0.000000	0.000000	0.000000	0.000000	0.000000	0.000000	0.000000	0.000000
2	2.76386	-4.726689E-03	0.000000	0.000000	0.000000	0.000000	0.000000	0.000000
	0.000000	0.000000	0.000000	0.000000	0.000000	0.000000	0.000000	0.000000
	0.000000	0.000000	0.000000	0.000000	0.000000	0.000000	0.000000	0.000000
3	3.68847	0.000000	-0.415087	0.000000	0.000000	0.000000	0.000000	0.000000
	0.000000	0.000000	0.000000	0.000000	0.000000	0.000000	0.000000	0.000000
	0.000000	0.000000	0.000000	0.000000	0.000000	0.000000	0.000000	0.000000
4	56.3301	0.000000	0.000000	-0.162461	60.4400	0.162461	0.000000	0.000000
	0.000000	0.000000	0.000000	0.000000	0.000000	0.000000	0.000000	0.000000
	0.000000	0.000000	0.000000	0.000000	0.000000	0.000000	0.000000	0.000000
5	1.790870E-03	0.000000	0.000000	0.000000	-2.633633E-02	0.000000	0.000000	0.000000
	0.000000	0.000000	0.000000	0.000000	0.000000	0.000000	0.000000	0.000000
	0.000000	0.000000	0.000000	0.000000	0.000000	0.000000	0.000000	0.000000
6	0.000000	0.000000	0.000000	0.178658	0.000000	-2.75950	0.000000	-0.342240
	160.549	0.000000	0.000000	0.000000	1.48931	0.000000	0.000000	0.000000
	0.000000	3.876588E-03	0.000000	0.000000	20.2884	-147.226	0.000000	0.000000
7	0.000000	0.000000	0.000000	0.000000	0.000000	0.000000	-2.58065	-0.342240
	160.549	0.000000	0.000000	0.000000	1.48931	0.000000	0.000000	0.000000
	0.000000	3.876588E-03	0.000000	0.000000	20.2884	-147.226	0.000000	0.000000
8	0.000000	0.000000	0.000000	3.280205E-02	0.000000	-6.940315E-02	8.948298E-02	-1.45482
	-38.7641	0.000000	0.000000	0.000000	4.987663E-02	0.000000	0.000000	0.000000
	0.000000	2.520934E-04	0.000000	-0.855545	1.24794	-8.37319	0.000000	0.000000
9	0.000000	0.000000	0.000000	1.532144E-04	0.000000	-1.532144E-04	1.010713E-03	-8.170790E-03
	-0.350000	0.000000	0.000000	0.000000	0.000000	0.000000	0.000000	0.000000
	0.000000	0.000000	0.000000	0.000000	0.000000	0.000000	0.000000	0.000000
10	0.000000	0.000000	0.000000	0.000000	0.000000	0.000000	0.000000	0.000000
	0.000000	0.000000	0.000000	0.000000	0.000000	0.000000	0.000000	0.000000
	0.000000	0.000000	0.000000	0.000000	0.000000	0.000000	0.000000	0.000000

Matrix A (continued)

11	0.000000	0.000000	0.000000	0.000000	0.000000	0.000000	0.000000	0.000000
	0.000000	0.000000	0.000000	0.000000	0.000000	0.000000	0.000000	0.000000
	0.000000	0.000000	0.000000	1.00000	0.000000	0.000000	0.000000	0.000000
12	0.000000	0.000000	0.000000	0.000000	0.000000	0.000000	0.000000	0.000000
	0.000000	0.000000	0.000000	0.000000	0.000000	0.000000	0.000000	0.000000
	0.000000	0.000000	0.000000	0.930171	0.000000	0.000000	0.000000	0.000000
13	0.000000	0.000000	0.000000	0.000000	0.000000	0.000000	0.000000	2.51040
	30.9211	0.000000	0.000000	0.000000	-0.497303	0.000000	0.000000	0.000000
	0.000000	4.442664E-04	0.000000	0.000000	1.32189	0.000000	0.000000	0.000000
14	0.000000	0.000000	0.000000	0.000000	0.000000	0.000000	0.000000	-0.391571
	183.691	0.000000	0.000000	0.000000	1.88748	2.331033E-02	-382.339	-7.070638E-08
	0.220903	-7.122380E-03	0.000000	0.000000	-16.3393	0.000000	0.000000	0.000000
15	0.000000	0.000000	0.000000	0.000000	0.000000	0.000000	0.000000	0.000000
	0.000000	0.000000	0.000000	0.000000	0.000000	1.611606E-04	-0.267913	0.000000
	0.000000	-1.624104E-06	0.000000	0.000000	0.000000	0.000000	0.000000	0.000000
16	0.000000	0.000000	0.000000	0.000000	0.000000	0.000000	0.000000	0.000000
	0.000000	0.000000	0.000000	0.000000	0.000000	3.330113E-02	-60.1633	-8.071343E-09
	0.000000	-3.460754E-04	0.000000	0.000000	1.29045	0.000000	0.000000	0.000000
17	0.000000	0.000000	0.000000	0.000000	0.000000	0.000000	0.000000	0.000000
	0.000000	0.000000	0.000000	0.000000	0.000000	0.000000	0.000000	0.000000
	-0.118022	1.477882E-03	0.000000	0.000000	0.000000	0.000000	0.000000	0.000000
18	0.000000	0.000000	0.000000	0.000000	0.000000	0.000000	0.000000	0.000000
	0.000000	0.000000	0.000000	0.000000	0.000000	3.58563	3382.65	-7.141252E-05
	0.000000	-0.129882	0.000000	0.000000	-28.5643	0.000000	0.000000	0.000000
19	0.000000	0.000000	0.000000	0.000000	0.000000	0.000000	0.000000	0.000000
	0.000000	0.000000	0.000000	0.000000	0.000000	0.000000	0.000000	0.000000
	0.000000	1.825349E-05	-0.454545	0.000000	0.000000	0.000000	0.000000	0.000000
20	0.000000	0.000000	0.000000	0.000000	0.000000	0.000000	0.000000	5.43010
	0.000000	0.000000	0.000000	-5.43010	0.000000	0.000000	0.000000	0.000000
	0.000000	0.000000	0.000000	-2.85714	0.000000	0.000000	0.000000	0.000000
21	0.000000	0.000000	0.000000	0.000000	0.000000	0.000000	0.000000	0.000000
	0.000000	0.000000	0.000000	0.000000	0.000000	0.000000	0.000000	0.000000
	0.000000	0.000000	0.000000	0.000000	-0.500000	0.000000	0.000000	0.000000

Matrix A (continued)

22	0.000000	0.000000	0.000000	0.000000	0.000000	0.000000	0.000000	0.000000
	0.000000	0.000000	0.000000	0.000000	0.000000	0.000000	0.000000	0.000000
	0.000000	1.144245E-06	0.000000	0.000000	3.103095E-02	-0.182832	0.000000	-3.960314E-04
23	0.000000	0.000000	0.000000	0.000000	0.000000	0.000000	0.000000	0.000000
	0.000000	0.000000	0.000000	0.000000	0.000000	0.000000	0.000000	0.000000
	0.000000	1.107950E-04	0.000000	0.000000	-0.250000	0.000000	-5.000000E-02	0.000000
24	0.000000	0.000000	0.000000	0.000000	0.000000	0.000000	0.000000	0.000000
	0.000000	0.000000	0.000000	0.000000	0.000000	0.000000	0.000000	0.000000
	0.000000	0.000000	0.000000	0.000000	0.000000	0.000000	2.127660E-02	-2.127660E-02

MATRIX B

1	0.000000	0.000000	0.000000	0.000000	0.000000
2	0.000000	0.000000	0.000000	0.000000	0.000000
3	0.000000	0.000000	0.000000	0.000000	0.000000
4	0.000000	0.000000	0.000000	0.000000	0.000000
5	0.000000	0.000000	0.000000	0.000000	0.000000
6	0.000000	0.000000	0.000000	0.000000	0.000000
7	0.000000	0.000000	0.000000	0.000000	0.000000
8	0.000000	0.000000	0.655545	0.000000	0.000000
9	0.000000	0.000000	0.000000	0.000000	0.000000
10	-3.256940E-04	0.000000	0.000000	0.000000	0.000000
11	0.000000	7.115836E-04	0.000000	0.000000	0.000000
12	0.000000	6.618943E-04	0.000000	0.000000	0.000000
13	0.000000	0.000000	0.000000	0.000000	0.000000
14	0.000000	0.000000	0.000000	0.000000	-2.15561
15	0.000000	0.000000	0.000000	0.000000	0.000000
16	0.000000	0.000000	0.000000	0.000000	-0.246070
17	0.000000	0.000000	0.000000	0.000000	0.000000
18	0.000000	0.000000	0.000000	0.000000	-2177.14
19	0.000000	0.000000	0.000000	0.000000	0.428516
20	0.000000	0.000000	0.000000	0.000000	0.000000
21	0.000000	0.000000	0.000000	0.500000	0.000000
22	0.000000	0.000000	0.000000	0.000000	0.000000
23	0.000000	0.000000	0.000000	0.000000	2.60101

Matrix B (continued)

24	0.000000	0.000000	0.000000	0.000000	0.000000

MATRIX C

1	1.00000	0.000000	0.000000	0.000000	0.000000	0.000000	0.000000	0.000000
	0.000000	0.000000	0.000000	0.000000	0.000000	0.000000	0.000000	0.000000
	0.000000	0.000000	0.000000	0.000000	0.000000	0.000000	0.000000	0.000000
2	0.000000	0.000000	0.000000	0.000000	0.000000	0.000000	0.000000	1.00000
	0.000000	0.000000	0.000000	0.000000	0.000000	0.000000	0.000000	0.000000
	0.000000	0.000000	0.000000	0.000000	0.000000	0.000000	0.000000	0.000000
3	0.000000	0.000000	0.000000	0.000000	0.000000	0.000000	0.000000	0.000000
	0.000000	0.000000	0.340136	0.000000	0.000000	0.000000	0.000000	0.000000
	0.000000	0.000000	0.000000	0.000000	0.000000	0.000000	0.000000	0.000000
4	0.000000	0.000000	0.000000	0.000000	0.000000	0.000000	0.000000	0.000000
	0.000000	0.000000	0.000000	0.000000	0.000000	0.000000	0.000000	5.545900E-02
	0.000000	0.000000	0.000000	0.000000	0.000000	0.000000	0.000000	0.000000
5	0.000000	0.000000	0.000000	0.000000	0.000000	0.000000	0.000000	0.000000
	0.000000	0.000000	0.000000	0.000000	0.000000	0.000000	0.000000	0.000000
	0.000000	1.935600E-04	0.000000	0.000000	0.000000	0.000000	0.000000	0.000000
6	0.000000	0.000000	0.000000	0.000000	0.000000	0.000000	0.000000	0.000000
	0.000000	0.000000	0.000000	0.000000	0.000000	0.000000	0.000000	0.000000
	0.000000	4.015767E-05	0.000000	0.000000	-1.00000	0.000000	0.000000	0.000000
7	0.000000	0.000000	0.000000	0.000000	0.000000	0.000000	0.000000	0.000000
	0.000000	0.000000	0.000000	0.000000	0.000000	0.000000	0.000000	0.000000
	0.000000	0.000000	1.00000	0.000000	0.000000	0.000000	0.000000	0.000000
8	0.000000	0.000000	0.000000	0.000000	0.000000	0.000000	0.000000	0.000000
	0.000000	0.000000	0.000000	1.00000	0.000000	0.000000	0.000000	0.000000
	0.000000	0.000000	0.000000	0.000000	0.000000	0.000000	0.000000	0.000000

DATFILE D

1	0.000000	0.000000	0.000000	0.000000	0.000000
2	0.000000	0.000001	0.000000	0.000000	0.000000
3	0.000000	0.000000	0.000001	0.000000	0.000000
4	0.000000	0.000000	0.000000	0.000000	0.000000
5	0.000000	0.000000	0.000000	0.000000	0.000001
6	0.001000	0.000000	0.000000	0.000001	0.942736
7	0.000000	0.000000	0.000000	0.000000	0.000000
8	0.000000	0.000000	0.000000	0.000000	0.000000

OPEN-LOOP POLES

Mode No.	Real Value	Imaginary Value
1	0.000000	0.000000
2	0.000000	0.000000
3	-2.905705E-08	0.000000
4	-7.035677E-07	0.000000
5	-1.969287E-03	0.000000
6	-1.135474E-02	0.000000
7	-2.726444E-02	0.000000
8	-4.323566E-02	1.301648E-02
9	-4.323566E-02	-1.301648E-02
10	-0.133131	-0.292423
11	-0.133131	0.292423
12	-0.156244	2.503049E-02
13	-0.156244	-2.503049E-02
14	-0.203958	9.462140E-02
15	-0.203958	-9.462140E-02
16	-0.357875	0.000000
17	-0.454545	0.000000
18	-0.500000	0.000000
19	-1.08537	0.000000
20	-1.81386	-2.59894
21	-1.81386	2.59894
22	-2.58611	0.000000
23	-2.80511	0.000000
24	-6.63056	0.000000

ISSN 0067 - 0367

To identify individual documents in the series we have assigned an AECL- number to each.

Please refer to the AECL- number when requesting additional copies of this document

from

Scientific Document Distribution Office
Atomic Energy of Canada Limited
Chalk River, Ontario, Canada
K0J 1J0

Price $5.00 per copy

ISSN 0067 - 0367

Pour identifier les rapports individuels faisant partie de cette série nous avons assigné un numéro AECL- à chacun.

Veuillez faire mention du numéro AECL- si vous demandez d'autres exemplaires de ce rapport

au

Service de Distribution des Documents Office
L'Energie Atomique du Canada Limitée
Chalk River, Ontario, Canada
K0J 1J0

Prix $5.00 par exemplaire

1481-84